Ocean Engineering 342 (2025) 123111

Contents lists available at ScienceDirect

Ocean Engineering

journal homepage: www.elsevier.com/locate/oceaneng

Research paper

Assessment of ship manoeuvring models for the development of a collision risk evaluation framework

E. Lotovskyi, L. Moreira, A.P. Teixeira *

Centre for Marine Technology and Ocean Engineering (CENTEC), Instituto Superior Técnico, Universidade de Lisboa, Portugal

ARTICLE INFO

Keywords:
Ship manoeuvring models
Hydrodynamic derivatives
Empirical regression models
Turning manoeuvre
Collision risk
Manoeuvring Modelling Group (MMG)
KVLCC2
KCS

ABSTRACT

Collision risk evaluation remains a critical concern with the intensification of maritime traffic. Although various methodologies exist for estimating vessel collision risk, relatively few provide a detailed explanation of the manoeuvrability characteristics of the vessels involved in the collision scenario. This paper assesses the accuracy and precision of empirical manoeuvrability models as well as the effect of their hydrodynamic derivatives and general vessel data on the ship trajectories. To achieve this, a vessel manoeuvring model is formulated based on the nonlinear dynamic equations of motion of the Manoeuvring Modelling Group (MMG) approach and validated using two benchmark ships. Furthermore, the study focuses on the assessment of turning manoeuvre parameters relevant to different collision risk levels, with particular emphasis on close-quarter situations. Attention is given to the accuracy and precision of standard and hybrid regression models, as well as to the sensitivity of the predicted turning trajectories with respect to general-propeller-rudder input data. The results identify the manoeuvring regression models best suited to modern tanker and container hull forms under varying simulation conditions, considering both model accuracy and input sensitivity. The findings contribute to the ongoing development of a comprehensive collision risk evaluation framework accounting for vessel manoeuvrability characteristics.

1. Introduction

With the increase in maritime traffic and the introduction of vessels with enhanced levels of automation expected in the near future, the issue of collision prevention is becoming increasingly critical (Abilio Ramos et al., 2019; Chaal et al., 2023; Fan et al., 2020). Various studies and methodologies have been proposed to estimate the probability and risk of vessel collisions (Čorić et al., 2021; Rong et al., 2022; Szlapczynski et al., 2018). However, few studies provide a detailed explanation of manoeuvrability characteristics in the assessment of collision risk and probability of collision (Lotovskyi and Teixeira, 2023; Montewka et al., 2010; Wang et al., 2020). Studies that incorporate manoeuvrability into collision risk assessments often present only the general mathematical formulation of the trajectory simulation model, while omitting critical details of how the manoeuvrability model is implemented. Such details are essential for evaluating the quality of the simulated manoeuvres, especially when collision-avoidance actions are modelled. Commonly overlooked aspects include the simplifications adopted, vessel type, propeller and rudder characteristics, hydrodynamic derivatives, among others.

This study aims to assess in more detail the empirical manoeuvrability models and their components, which can serve as a foundation for developing a more advanced collision risk evaluation model. Given the complexity of the subject, the scope of this article is limited to hydrodynamic derivatives. This focus reflects the study's role as the first published contribution to an ongoing effort to develop a comprehensive collision risk evaluation framework that explicitly incorporates vessel manoeuvrability characteristics.

Accurate ship manoeuvring predictions depend heavily on the choice of empirical models for hydrodynamic derivatives. In this context, hydrodynamic derivatives refer to the coefficients in the equations of motion that quantify how hydrodynamic forces and moments acting on a vessel vary with respect to changes in motion variables such as sway velocity, yaw rate and acceleration. These derivatives are fundamental components of manoeuvring models and play a critical role in accurately predicting a vessel's response to control inputs and external influences, including rudder actions and environmental forces.

Pires da Silva et al. (2023) conducted a sensitivity analysis of the

* Corresponding author.
E-mail address: teixeira@centec.tecnico.ulisboa.pt (A.P. Teixeira).

https://doi.org/10.1016/j.oceaneng.2025.123111
Received 27 June 2025; Received in revised form 14 September 2025; Accepted 6 October 2025
Available online 13 October 2025

total hydrodynamic forces and moments, as well as separately analysing the linear and non-linear polynomial regression model components, without incorporating any empirical model for hydrodynamic derivative estimation. Sutulo and Guedes Soares (2019) performed a numerical study combining various empirical hydrodynamic models of hull and rudder sub-models to determine the most accurate ones for simulating standard manoeuvres under adverse weather conditions. Sukas et al. (2019) conducted a sensitivity analysis of hydrodynamic derivatives and rudder parameters in a ship manoeuvring simulation model developed by integrating empirical formulas from multiple pre-existing models into a unified framework. The same principle was applied by Taimuri et al. (2020) with the objective of constructing a manoeuvrability model to assess the behaviour of ships in both deep and shallow waters.

This paper identifies the key components of the mathematical manoeuvrability model that significantly influence a ship's manoeuvring behaviour, with a focus on various turning manoeuvre metrics relevant to the ongoing development of a comprehensive collision risk assessment model. Additionally, different combinations of ship manoeuvring regression models for hydrodynamic derivatives with linear and nonlinear components are assessed in terms of accuracy and precision. Moreover, sensitivities are calculated to analyse the impact of the chosen polynomial regression model on turning manoeuvre parameters. For result validation, two benchmark ships, KVLCC2 and KCS, are used.

2. Literature review

Understanding a vessel's manoeuvring characteristics is crucial for collision probability assessment (Krata and Montewka, 2015; Lotovskyi et al., 2024), ship manoeuvring performance prediction at the design phase (Araújo et al., 2021; Cho et al., 2007; IMO, 2002), and the development of ship-handling simulators (Jensen et al., 2018; Senol and Seyhan, 2024). The manoeuvrability properties of a vessel can be assessed through sea trials or estimated using mathematical modelling techniques and machine learning algorithms (Moreira and Guedes Soares, 2022, 2024).

Ship manoeuvrability and collision risk are strongly interrelated in maritime navigation, particularly in collision evasive manoeuvres. When a vessel initiates an evasive manoeuvre to avoid other ships, the associated collision risk dynamically changes. This is primarily due to the vessel's large inertia and significant response delay, which can lead to underestimation of collision risk if manoeuvrability is neglected (Li et al., 2021). Consequently, ship manoeuvrability is a critical factor influencing navigational decision-making, as the success of any evasive action depends largely on the vessel's manoeuvring characteristics.

Several studies have incorporated manoeuvrability into collision risk assessment. Li et al. (2019) derived collision risk parameters based on manoeuvring performance to address multi-ship collision avoidance. Gil (2021) examined ship allision in close-quarters situations, using manoeuvrability and Minimum Distance to Collision (MDTC) as risk parameters. Hörteborn and Ringsberg (2021) proposed a methodology integrating Automatic Identification System (AIS) data with a commercial ship manoeuvring simulator to model marine traffic schemes and assess allision probabilities. Furthermore, Li et al. (2021) combined manoeuvrability, International Regulations for Preventing Collisions at Sea (COLREG), good seamanship practices and conflict risk assessment in a practical methodology that defines available room-for-manoeuvre and recommends evasive actions in multiple-ship encounters.

Various mathematical models have been proposed to assess ship manoeuvring characteristics. One of the simplest models is the rudder-to-yaw response model, commonly referred to as the Nomoto model (Nomoto et al., 1957). This model describes the ship's rate of turn in response to a given rudder angle and is frequently used in collision risk studies (Baldauf et al., 2015; Lotovskyi and Teixeira, 2023; Mehdi et al., 2020; Silveira et al., 2016). However, the Nomoto model exhibits limited predictive accuracy when applied to comprehensive manoeuvring simulations that account for speed reduction and the ship's trajectory (Sutulo and Guedes Soares, 2024).

To accurately describe the full manoeuvring behaviour of a ship, more advanced physically-based models should be adopted, such as the Abkowitz-type model (also referred to as the whole-ship model) and the component-based model. In the Abkowitz-type model, the hull, rudder and propeller are treated as a single rigid body, with the equations of motion expressed by a third-order Taylor series expansion (Abkowitz, 1964). In contrast, the component-based model considers the hull, rudder, and propeller as distinct elements, computing their respective forces and moments separately before summing them to determine the total force and moment acting on the vessel.

The Manoeuvring Modelling Group (MMG) model, introduced at the Japanese Towing Tank Conference (JTTC) in 1977, is the most well-known component-based model (Yasukawa and Yoshimura, 2015). The Japan Society of Naval Architects and Ocean Engineers later refined it, reviewing key aspects to enhance accuracy, simplicity and adaptability, leading to the MMG standard method for ship manoeuvring simulations.

Regardless of the mathematical model employed, the accurate determination of hydrodynamic derivatives in the equations of motion is essential for predicting the manoeuvring performance of a marine vehicle (Balagopalan et al., 2020). The hydrodynamic derivatives are regression coefficients in the Taylor series expansion of the hydrodynamic forces and moments. While they lack direct physical meaning, their primary function is to ensure mathematical accuracy, providing a smooth and consistent representation of the hydrodynamic forces (Fossen, 2011). Hydrodynamic derivatives, which are specific to each vessel, can be determined through several methods: captive model test (Islam and Guedes Soares, 2018; Yeo et al., 2018), computational fluid dynamics (CFD) calculation (Aram and Silva, 2019; Go and Ahn, 2019), identification from free-running model tests (Yun et al., 2018) or full-scale trials, real-time identification procedure (Iseki, 2019), and reference databases of hydrodynamic derivatives. However, among the methods, the empirical estimation remains a rapid and cost-effective alternative when data availability is limited, time constraints are present, or financial resources are restricted (ITTC, 2008).

Smitt (1971) and Norrbin (1971) estimated linear hydrodynamic derivatives by regression analyses on nearly 30 datasets from planar motion mechanism tests. However, it is insufficient to analyse ship manoeuvring solely through the linear terms of the forces, particularly when the vessel is manoeuvring with large rudder angles (Inoue et al., 1981). In such cases, the non-linear terms become the predominant factors influencing the manoeuvring behaviour. Inoue et al. (1981) deducted linear and non-linear coefficients and accounted for various load conditions, including trim. Later, Kijima et al. (1990) revised Inoue et al. (1981) formulas and proposed a comprehensive set of prediction models based on the MMG-type mathematical framework. Yoshimura and Masumoto (2011), based on their own hydrodynamic database and Kijima et al. (1990), developed empirical models for estimating hydrodynamic derivatives specific to medium-to high-speed merchant ships and fishing vessels. More recently, Sutulo and Guedes Soares (2019) proposed mathematical expressions for hydrodynamic derivatives derived from Inoue et al. (1981) nonlinear manoeuvring derivative plots.

Nearly all papers cited in this paper that refer to empirical equations for hydrodynamic derivatives were either developed in the late 20th century or built upon work from that period. At the time, full-bodied bulk carriers and tankers were the predominant vessel types on major shipping routes, leading to empirical methods that are generally applicable only to these ships (Yoshimura and Masumoto, 2011). Consequently, there is a need for alternative models tailored to other vessel types. However, accessing more recent studies remains challenging, as much of the research is often confidential due to commercial interests.

The empirical equations presented in this paper offer a rapid and practical means of estimating hydrodynamic derivatives for simulation

purposes. However, it is important to recognise that empirical methods have limitations in delivering reliable manoeuvrability predictions (ITTC, 2008). For instance, their accuracy tends to decrease in shallow water conditions. Additionally, many of these models do not incorporate specific hull form details, such as aft body (Oltmann, 2003), which are often crucial for assessing manoeuvrability (Aoki et al., 2006).

Despite the limitations, the accuracy requirements for manoeuvrability prediction are generally less rigorous than those for resistance and propulsion studies, with deviations of up to 15 % considered acceptable (Sutulo and Guedes Soares, 2019). Furthermore, from a qualitative perspective, the empirical methods typically provide reliable estimates of how specific parameters influence the behaviour of the hull, propulsion system and steering device. As such, more comprehensive information regarding the performance and limitations of the empirical methods, as well as a deeper understanding of the relative significance of their elements and components, are necessary to enhance their predictive capabilities.

Accordingly, the objective of this paper is to investigate the performance and limitations of empirical manoeuvrability models by analysing their underlying components and evaluating their predictive accuracy, as well as identifying the most influential parameters on their overall performance. The ultimate goal is to contribute to the development of a robust collision risk assessment framework.

The paper is structured as follows. Section 3 presents the methodology, beginning with a description of the implemented model used in this study. This is followed by the mathematical formulation of the vessel manoeuvring model based on the MMG procedure, which includes sub-models for the hydrodynamic longitudinal force of the propeller, the hydrodynamic forces and moments acting on the rudder and the hydrodynamic forces and moments acting on the hull. Additionally, empirical models for estimating hydrodynamic derivatives are briefly introduced.

Since different turning circle parameters are required depending on the implemented collision risk level, the distinctions between approaches are clarified in a dedicated subsection. The final subsection introduces the reliability assessment tools used in this study and presents the benchmark ships.

Section 4 is dedicated to Results and Discussion. Here, the mathematical model is validated based on known results of the benchmark ships. Accuracy and precision assessments are then conducted to determine the most suitable polynomial regression model for estimating hydrodynamic derivatives. Furthermore, a sensitivity assessment is performed to analyse the influence of input data and the impact of the chosen polynomial regression model on turning manoeuvre parameters. This analysis provides deeper insight into ship behaviour across different encounter scenarios based on manoeuvrability principles. Finally, Section 5 summarises the main conclusions of the paper.

3. Methodology

3.1. Framework description

One of the reasons why manoeuvrability is often overlooked in collision probability assessments is the limited availability of hydrodynamic data for ships. However, the integration of manoeuvrability into such assessments can be enhanced if hydrodynamic data are estimated using empirical formulations. To develop a robust model for analysing the collision probability and risk, it is essential to first assess the quality of the input data used for vessel manoeuvrability simulations. This assessment provides an understanding of how deviations in parameters can influence trajectory predictions, which is especially important when vessel data are limited and must be estimated empirically.

The vessel manoeuvrability simulation and assessment framework proposed in this paper represents an initial step in developing a comprehensive collision risk evaluation model based on the manoeuvring characteristics of the vessels. A global overview of the approach is presented in Fig. 1. The input data used for vessel manoeuvrability simulation is divided into two sub-groups: hydrodynamic derivatives data and general-propeller-rudder data. This data is then processed through the Vessel Manoeuvring Model (VMM), with its mathematical formulation outlined in Section 3.2. The VMM generates the vessel's turning trajectory, along with key manoeuvring parameters such as advance, transfer, tactical diameter, among others (see Section 3.4). A reliability assessment sub-model further evaluates the output turning circle data, enabling conclusions regarding the accuracy and precision of polynomial regression models and input data elasticity. It is expected that these findings lay as the groundwork for the subsequent development of a collision assessment model.

The separation of input data into two distinct sets allows for a focused assessment of hydrodynamic derivatives. Hydrodynamic derivatives are regression coefficients without direct physical interpretation that can be estimated empirically using polynomial regression models. These models may include both linear and nonlinear coefficients or solely linear coefficients. This study evaluates ten polynomial regression models: five incorporating both linear and nonlinear coefficients (Inoue et al., 1981; Kijima et al., 1990; Matsunaga, 1993; Yoshimura and Ma, 2003; Yoshimura and Masumoto, 2011) and five consisting of only linear coefficients (Ankudinov, 1987; Clarke et al., 1983; Khattab, 1984; Norrbin, 1971; Smitt, 1971). Inoue et al. (1981) indicated that models relying solely on linear coefficients are insufficient for accurately analysing ship manoeuvrability. Therefore, this study aims to assess each regression model with both linear and nonlinear coefficients, and the impact of integrating regression models with only linear coefficients into models with both linear and nonlinear coefficients by substitution of the linear coefficients of the latter models with linear coefficients of the former models. Consequently, 5 standard polynomial regression models and 25 hybrid polynomial regression models are analysed. The differences in accuracy and precision between polynomial regression models are examined. The empirical expressions of all polynomial regression models implemented in the VMM are summarised in Appendix B.

While hydrodynamic derivatives must be examined as a cohesive set, the general-propeller-rudder data can be analysed on a variable-by-variable basis, as their empirical formulations may originate from different sources. Table 1 provides a summary of all input variables within the general-propeller-rudder data set, categorised into general-related data, propeller-related data and rudder-related data.

The Vessel Manoeuvring Model (VMM) is a mathematical model based on the nonlinear dynamic equations of motion for a rigid body with three degrees of freedom (DOF). It simulates the turning circle manoeuvre, providing both the ship's trajectory and the main manoeuvring parameters (see Section 3.4). The model incorporates original benchmark ship data as well as experimental results from turning circle manoeuvres of benchmark ships. In Section 4.1, the mathematical model implemented in the VMM is validated for both benchmark ships, KVLCC2 and KCS.

At present, the VMM is capable of simulating turning manoeuvres using general-propeller-rudder input data. This paper represents the first study developed within the broader scope of constructing a collision risk evaluation model. As an initial step, the VMM is designed to estimate hydrodynamic derivatives empirically. To achieve this, the VMM includes a function that integrates various empirical polynomial regression models.

VMM is designed for single-screw ships operating in deep water under calm conditions, without external disturbances such as wind or currents. Besides, VMM is based on the following assumptions:

1. The ship behaves as a rigid body;
2. Hydrodynamic forces acting on the vessel are assumed to be quasi-steady;
3. The lateral velocity component is negligible compared to the longitudinal velocity component.

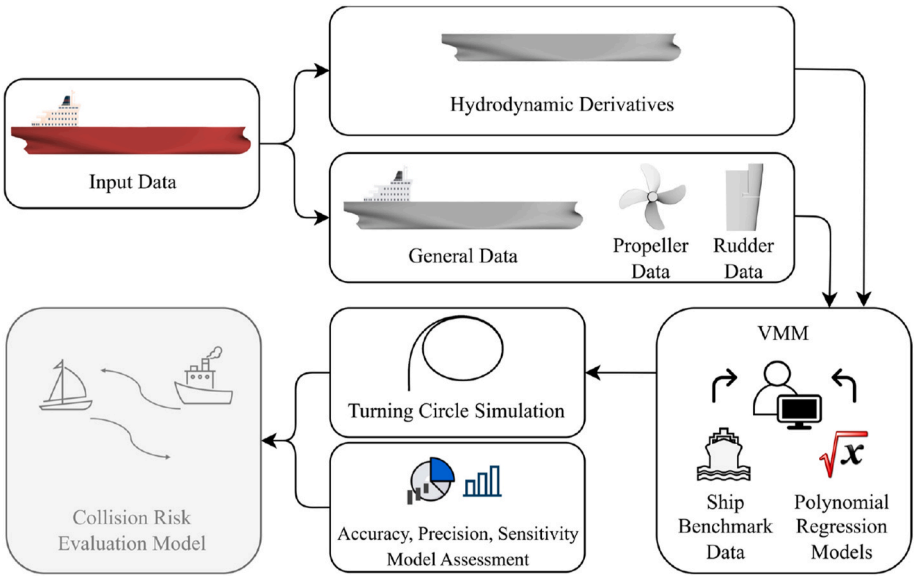

Fig. 1. Vessel manoeuvrability simulation and assessment framework.

Table 1
Summary of general-propeller-rudder input data.

Input data		
General data	Propeller data	Rudder data
$m, x_G, R'_0, \mu_{11}, \mu_{22}, \mu_{26}, \mu_{66}$	$a_0, a_1, a_2, n_P, t_P, w_{P_0}, D_P$	$a_H, l'_R, t_R, w_{R_0}, x'_H, A_R, H_R, \gamma_R, \varepsilon, \kappa, \Lambda$

4. Wave-making effects are neglected.
5. The impact of roll coupling on manoeuvring is considered insignificant.

Future studies are expected to extend the capabilities of the VMM, enabling it to simulate complete collision avoidance trajectories based on minimal input data.

Each input data set is analysed separately. The performance of different empirical models is assessed in terms of accuracy and precision, particularly in the case of hydrodynamic derivatives. Additionally, the effect of model hybridisation is examined. For the second input data set (i.e., general-propeller-rudder data), the study evaluates the influence of individual input variables on turning manoeuvre parameters and identifies the most critical variables for accurate manoeuvreability estimation.

3.2. Mathematical formulation of vessel manoeuvring model

3.2.1. Dynamic equations of motion

Based on Newtonian mechanics, the nonlinear dynamic equations of motion for a rigid body (i.e., surface vessel) with 3 degrees of freedom (3-DOF) moving in the horizontal plane is presented on the left side of Equation (1). Besides, this mathematical model excludes environmental disturbances like wind, waves and currents.

$$\begin{bmatrix} (m+\mu_{11})\dot{u} - mvr - mx_G r^2 \\ (m+\mu_{22})\dot{v} + (mx_G+\mu_{26})\dot{r} + mur \\ (mx_G+\mu_{26})\dot{v} + (I_{zz}+\mu_{66})\dot{r} + mx_G ru \end{bmatrix} = \begin{bmatrix} X_H + X_R + X_P \\ Y_H + Y_R \\ N_H + N_R \end{bmatrix} \quad (1)$$

The origin of the mathematical model described in Equation (1) is located at the midship section on the centreline of the ship. The origin of the reference is not at the centre of gravity, because its longitudinal position typically varies under different loading conditions, which in turn alters the coordinates of the rudder and propeller positions, thereby increasing the complexity of the simulation (Yasukawa and Yoshimura, 2015). The quasi-steady forces and moments are assessed based on the individual open water characteristics of the hull, propeller and rudder, as well as their interaction components, as represented on the right side of Equation (1), where: X_H, Y_H and N_H are quasi-steady forces and moment acting on ship hull in surge, sway and yaw, respectively; X_R, Y_R and N_R are quasi-steady forces and moment acting on rudder in surge, sway and yaw, respectively; X_P is surge force caused by the propeller. It is important to note that side force, Y_P, and yaw moment, N_P, due to propeller are neglected as they have smaller magnitudes compared to those of hull and rudder components.

The mass moment of inertia of a vessel relative to a vertical axis can be estimated as follows (SNAME, 1989):

$$I_{ZZ} = 0.0625\, m\, L_{PP}^2 \quad (2)$$

At any given instant of time t, the vessel's position is described by the coordinates of the body-fixed frame origin, C, which include the

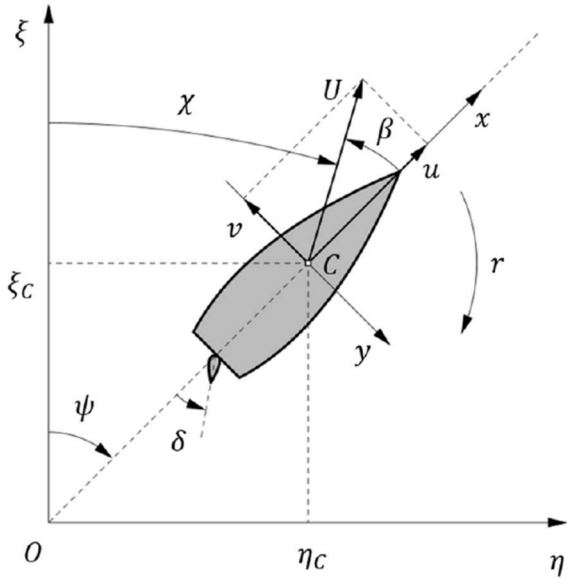

Fig. 2. Coordinate system: axes fixed relative to the Earth, $O\xi\eta$, and axes fixed in the ship, Cxy.

advance, $\xi_c(t)$, transfer, $\eta_c(t)$, and heading (yaw) angle, $\psi(t)$, which is positive in the clockwise direction (see Fig. 2). The ship's motion is characterised by its instantaneous velocity, $U(t)$, which includes the surge velocity, $u(t)$, and sway velocity, $v(t)$, as components along the body-fixed axes, see Equation (3), as well as the yaw rate, $r(t)$.

$$U^2 = u^2 + v^2 \tag{3}$$

The kinematic differential equations for the generalised coordinates are:

$$\begin{cases} \dot{\xi}_C = u\cos(\psi) - v\sin(\psi) \\ \dot{\eta}_C = u\sin(\psi) + v\cos(\psi) \\ \dot{\psi} = r \end{cases} \tag{4}$$

The manoeuvring simulation problem represents limited sensitivity to the choice of integration method. Thus, advanced integration schemes, such as the Fourth-Order Runge-Kutta method, offer minimal advantage for solving the ship's equations of motion (Barr, 1993). Therefore, in this paper, the Euler integration method is employed.

3.2.2. Nondimensional representation

In line with standard practices in ship hydrodynamic analysis, several procedures and results are presented in nondimensional form where appropriate. Nondimensional metrics are denoted by a single prime symbol, ($'$). Unless otherwise specified, the reference quantities for nondimensionalisation include water density, ρ, length of the vessel measured between perpendiculars, L_{PP}, draught, d, and speed, U. In this study, the nondimensional equations applied to ship and kinematic metrics are based on SNAME "prime" system (see Table 2) used with the reference area $L_{PP}\,d$ suggested by the wing analogy (Norrbin, 1971).

3.2.3. Sub-model of hydrodynamic longitudinal force of propeller

The rotation of a propeller generates forward thrust, commonly referred to as the surge force, which propels a vessel along its axis. This force arises from the pressure difference between the front and back surfaces of the propeller blades as they move through the water. Mathematically, the surge force produced by a propeller, X_P, is expressed as follows (Yasukawa and Yoshimura, 2015):

$$X_P = (1 - t_P)\,T_P \tag{5}$$

where, t_P is the thrust deduction coefficient and T_P is the propeller thrust force.

Typically, mathematical models neglect the sway force, Y_P, and yaw moment, N_P, generated by the propeller. This simplification is valid for most merchant ships, except when the modelling of stopping manoeuvres is required (Sutulo and Guedes Soares, 2019).

Table 2
Nondimensional equations for ship and kinematic metrics.

Metrics	Nondimensional equations			
Yaw rate	$r' = \frac{r\,L_{PP}}{U}$			
Velocity	$v' = \frac{v}{U}$			
Longitudinal distance	$x'_G = \frac{x_G}{L_{PP}}$	$x'_P = \frac{x_P}{L_{PP}}$	$x'_H = \frac{x_H}{L_{PP}}$	
Moment	$N' = \frac{N}{\frac{1}{2}\rho\,L_{PP}^2\,d\,U^2}$			
Force	$X' = \frac{X}{\frac{1}{2}\rho\,L_{PP}\,d\,U^2}$	$Y' = \frac{Y}{\frac{1}{2}\rho\,L_{PP}\,d\,U^2}$		
Mass	$m' = \frac{m}{\frac{1}{2}\rho\,L_{PP}^2\,d}$			
Added mass	$\mu'_{11} = \frac{\mu_{11}}{\frac{1}{2}\rho\,L_{PP}^2\,d}$	$\mu'_{22} = \frac{\mu_{22}}{\frac{1}{2}\rho\,L_{PP}^2\,d}$	$\mu'_{26} = \frac{\mu_{26}}{\frac{1}{2}\rho\,L_{PP}^3\,d}$	$\mu'_{66} = \frac{\mu_{66}}{\frac{1}{2}\rho\,L_{PP}^4\,d}$

The accurate value of propeller thrust requires extensive model testing. To simplify the procedure, dimensionless propeller coefficients have been introduced, defined in terms of water density, ρ, number of propeller revolutions, n_P, and propeller diameter, D_P. The two most significant coefficients, used in this research, are the propeller advance coefficient, J_P, and propeller thrust open water characteristic, K_T. Thus, the propeller thrust force, T_P, is expressed by (Yasukawa and Yoshimura, 2015):

$$T_P = \rho\,n_P^2\,D_P^4\,K_T(J_P) \tag{6}$$

The simulation of standard definitive manoeuvres is typically performed under the assumption of a constant propeller rotation rate, n_P (Barr, 1993).

Propeller thrust open water characteristic, K_T, can be expressed as the 2nd polynomial function of propeller advanced ratio, J_P (Yasukawa and Yoshimura, 2015):

$$K_T(J_P) = a_2\,J_p^2 + a_1\,J_P + a_0 \tag{7}$$

$$J_P = \frac{u\,(1 - w_P)}{n_P\,D_P} \tag{8}$$

where, a_2, a_1, a_0 are coefficients of propeller thrust open water characteristic; u is surge velocity; w_P is wake fraction coefficient at the propeller position in manoeuvring motions.

To calculate the wake fraction coefficient, several procedures have been presented (Sutulo and Guedes Soares, 2019; Yasukawa and Yoshimura, 2015). In this study, the following expression is used:

$$w_P = w_{P_0}\,\exp\left(-4\,\beta_P^2\right) \tag{9}$$

where, w_{P_0} is the effective wake fraction coefficient at the propeller position in a straight forward motion and β_P is geometrical inflow angle to the propeller in manoeuvring motions (see Equations (10) and (11)).

$$\beta_P = \beta - x'_P\,r' \tag{10}$$

$$\beta = -\sin^{-1}\left(\frac{v}{U}\right) \tag{11}$$

where, β is hull drift angle, x'_P is the non-dimensional longitudinal coordinate of propeller position, r' is the non-dimensional yaw rate, v is the swaying velocity and U is the speed of the vessel.

If the longitudinal position of the propeller is unknown, it can be assumed that (Schneekluth, 1987):

$$x_P = (-0.5 + 0.04)\,L_{PP} \tag{12}$$

3.2.4. Sub-model of hydrodynamic forces and moment acting on the rudder

To model the effective rudder forces X_R, Y_R and moment N_R, this study adopts the framework proposed by Yasukawa and Yoshimura (2015):

$$\begin{aligned} X_R &= -(1 - t_R)\,F_N\sin(\delta) \\ Y_R &= -(1 + a_H)\,F_N\cos(\delta) \\ N_R &= -(x_R + a_H\,x_H)\,F_N\cos(\delta) \end{aligned} \tag{13}$$

where, F_N is the rudder normal force; δ is the rudder deflection angle; x_R is the longitudinal position of the rudder (see Fig. 3); t_R, a_H and x_H are hydrodynamic interaction coefficients between the ship hull and rudder, where t_R is the steering resistance deduction factor, a_H is the rudder force increase factor and x_H is the longitudinal position of an additional lateral force component.

If the longitudinal position of the rudder is unknown, it can be assumed that (Schneekluth, 1987):

$$x_R = -0.5\,L_{PP} \tag{14}$$

The rudder force increase factor, a_H, and the position of an additional

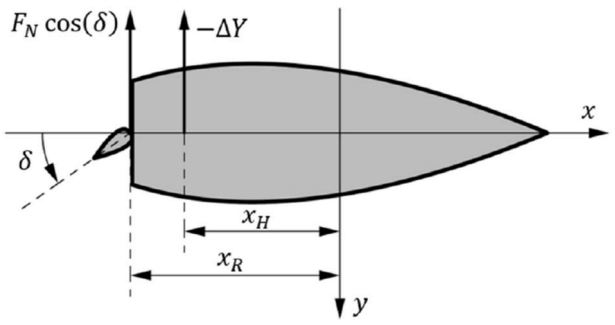

Fig. 3. Schematic representation of rudder force and additional lateral force induced by steering.

lateral force component, x_H, are derived from the hydrodynamic interaction between the ship hull and the rudder. This interaction is often modelled analogously to the behaviour of a wing with a flap, where the hull represents the main wing and the rudder acts as the flap (Yasukawa and Yoshimura, 2015). When the rudder is steered, it generates both a lift force on itself and an additional force, ΔY, on the ship's hull. The additional force arises from the hydrodynamic interplay between the hull (the main wing) and the rudder (the flap). Based on this interaction, a_H is defined as $-\Delta Y / F_N \cos(\delta)$ and the position x_H denotes the point of action of ΔY. To better illustrate this hydrodynamic interaction, Fig. 3 provides a schematic representation of the rudder force and the additional lateral force induced by steering.

According to MMG, as detailed by Yasukawa and Yoshimura (2015), the rudder normal force, F_N, is expressed as:

$$F_N = \frac{1}{2}\,\rho\, A_R\, U_R^2\, f_\alpha \sin(\alpha_R) \tag{15}$$

where, ρ is the water density, A_R is the lateral area of the rudder, U_R is the resultant inflow velocity to rudder (see Equation (16)), f_α is the gradient of the lift coefficient of the rudder, α_R is the effective inflow angle to the rudder (see Equation (17)).

$$U_R = \sqrt{u_R^2 + v_R^2} \tag{16}$$

$$\alpha_R = \delta - \frac{v_R}{u_R} \tag{17}$$

where, u_R and v_R are the longitudinal and lateral inflow velocity components to the rudder, respectively.

The rudder's geometric aspect ratio enables the estimation of the lift coefficient gradient, f_α, expressed as (Fujii, 1960):

$$f_\alpha = \frac{6.13\,\Lambda}{2.25 + \Lambda} \tag{18}$$

Fig. 4 provides a schematic representation of the rudder inflow angle and velocity, illustrating the longitudinal and lateral components of the velocity, too.

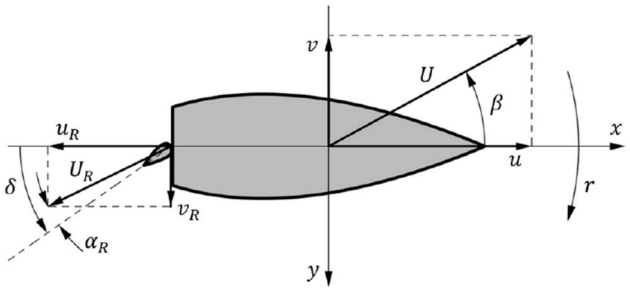

Fig. 4. Schematic representation of rudder inflow velocity and angle.

Longitudinal inflow velocity component to rudder, u_R, is expressed as:

$$u_R = \varepsilon\, u\,(1 - w_R)\sqrt{\eta\left(1 + \kappa\left(\sqrt{1 + \frac{8\,K_T}{\pi\, J_P^2}} - 1\right)\right)^2 + (1 - \eta)} \tag{19}$$

where, ε is the ratio of wake fraction at the propeller and rudder positions, w_R is the rudder wake fraction coefficient (see Equation (20)), κ is the experimental constant for expressing the longitudinal inflow velocity component to the rudder, η is the ratio of propeller diameter to rudder span (see Equation (21)).

$$w_R = w_{R_0} \exp\left(-4\,\beta_P^2\right) \tag{20}$$

$$\eta = \frac{D_P}{H_R} \tag{21}$$

Lateral inflow velocity component to rudder, v_R, is expressed as:

$$v_R = U\,\gamma_R\,\beta_R \tag{22}$$

where, γ_R is the flow straightening coefficient and β_R is effective inflow angle to the rudder in manoeuvring motions, expressed as:

$$\beta_R = \beta - l_R'\, r' \tag{23}$$

where, l_R' is an experimental constant used to accurately express v_R, which can be determined through captive model testing.

3.2.5. Sub-model of hydrodynamic forces and moment acting on the hull

The hydrodynamic forces and moment acting on ship hull are expressed as follows:

$$\begin{aligned} X_H &= \frac{1}{2}\,\rho\, L_{PP}\, d\, U^2\, X_H' \\ Y_H &= \frac{1}{2}\,\rho\, L_{PP}\, d\, U^2\, Y_H' \\ N_H &= \frac{1}{2}\,\rho\, L_{PP}^2\, d\, U^2\, N_H' \end{aligned} \tag{24}$$

Based on the third-order truncated Taylor series expansion for X_H', Y_H' and N_H' as proposed by Abkowitz (1964), this study employs a mathematical approach to estimate the nondimensional hydrodynamic forces and moment acting on the hull.

3.3. Empirical models for hydrodynamic derivatives estimation

For most ships, the forces acting on the hull during a manoeuvre can be approximated using multivariate Taylor series. For simplicity reason, it is assumed that any dimensionless quasi-steady hull force component depends only on the velocities of sway and yaw; besides, in most implementations, it is common to not exceed the power terms of three (Sutulo and Guedes Soares, 2011). Hence, considering that a ship is symmetric with respect to the centre plane, the third-order polynomial regression model of forces and moment acting on the hull is given by:

$$\begin{aligned} X_q'(v', r') &= X_0' + X_{vv}'(v')^2 + X_{rr}'(r')^2 + X_{vr}'(v'\,r') \\ \Phi_q'(v', r') &= \Phi_v' v' + \Phi_r' r' + \Phi_{vvv}'(v')^3 + \Phi_{vvr}'(v')^2 r' \\ &\quad + \Phi_{vrr}' v'(r')^2 + \Phi_{rrr}'(r')^3, \text{ where } \Phi = Y, N \end{aligned} \tag{25}$$

The regression coefficients of the model are called hydrodynamic derivatives. These coefficients, usually, are estimated from experiment. Besides, in some studies, the cubic terms are replaced with quadratic ones but with the absolute value function applied. However, this modification does not have any sensible advantages or drawbacks compared to the normal polynomial models and the choice is arbitrary.

Polynomial regression model used by Yasukawa and Yoshimura (2015), Yoshimura and Ma (2003) and Yoshimura and Masumoto (2011) are accordingly formulated as:

$$\begin{aligned} X'_H &= -R'_0 + X'_{vv}(v')^2 + X'_{vr}v'r' + X'_{rr}(r')^2 + X'_{vvvv}(v')^4 \\ Y'_H &= Y'_v v' + Y'_r r' + Y'_{vvv}(v')^3 + Y'_{vvr}(v')^2 r' + Y'_{vrr}v'(r')^2 + Y'_{rrr}(r')^3 \\ N'_H &= N'_v v' + N'_r r' + N'_{vvv}(v')^3 + N'_{vvr}(v')^2 r' + N'_{vrr}v'(r')^2 + N'_{rrr}(r')^3 \end{aligned} \tag{26}$$

Modified polynomial regression model can be found in the studies of Inoue et al. (1981), Kijima et al. (1990), Matsunaga (1993). In Inoue et al. (1981) the hydrodynamic force and moment expressions are accordingly formulated as:

$$\begin{aligned} X'_H &= -R'_0 + X'_{vr}v'r' \\ Y'_H &= Y'_v v' + Y'_r r' + Y'_{v|v|}v'|v'| + Y'_{r|r|}r'|r'| + Y'_{v|r|}v'|r'| \\ N'_H &= N'_v v' + N'_r r' + N'_{r|r|}r'|r'| + N'_{vvr}(v')^2 r' + N'_{vrr}v'(r')^2 \end{aligned} \tag{27}$$

In Kijima et al. (1990) and Matsunaga (1993), the hydrodynamic force and moment expressions are accordingly formulated as:

$$\begin{aligned} X'_H &= -R'_0 + X'_{vr}v'r' \\ Y'_H &= Y'_v v' + Y'_r r' + Y'_{v|v|}v'|v'| + Y'_{r|r|}r'|r'| + Y'_{vvr}(v')^2 r' + Y'_{vrr}v'(r')^2 \\ N'_H &= N'_v v' + N'_r r' + N'_{v|v|}v'|v'| + N'_{r|r|}r'|r'| + N'_{vvr}(v')^2 r' + N'_{vrr}v'(r')^2 \end{aligned} \tag{28}$$

3.4. Turning circle manoeuvre parameters and collision risk levels

The turning circle manoeuvre is a key manoeuvrability test required by classification societies during sea trials (ABS, 2006). The primary objective of this test is to evaluate a vessel's turning capability using a hard-over rudder. The manoeuvre must be conducted to both starboard and portside with a rudder angle not exceeding 35°. During trials, the vessel must complete a turning circle of at least 720°. This manoeuvre provides critical data on manoeuvring parameters, including advance, transfer, tactical diameter, turn diameter, time required to change course by 90° and 180°, speed loss, drift in a steady turn and both peak and final yaw rates (see Fig. 5).

The turning circle manoeuvre measurements required by classification societies are crucial for selecting the empirical model that best predicts a vessel's behaviour, ensuring the closest possible match to real performance. These measurements enable comparisons between true values available in the literature and the results obtained from simulations. However, not all of these measurements are equally relevant for assessing the risk of collision. The quality of the polynomial regression models varies as the heading angles change during turning circle manoeuvres. Therefore, when simulating more complex collision-avoidance manoeuvres, more turning parameters need to be considered during the validation process.

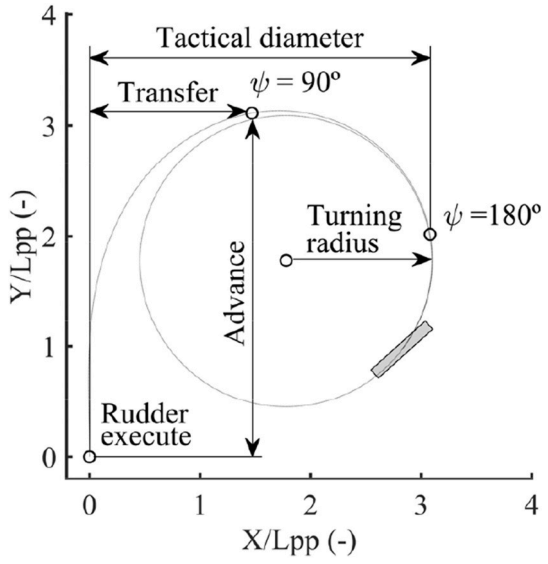

Fig. 5. Path of midship point in turning circle and main parameters of turning manoeuvre.

Collision avoidance at sea is a decision-making process in which the navigator takes timely and appropriate action in accordance with the COLREG rules, ensuring that vessels pass each other at a safe distance (Mohovic et al., 2021). When two ships are in sight of one another and a risk of collision exists, four stages of action can be distinguished: (i) free manoeuvre, (ii) action required by the give-way vessel, (iii) action permitted for the stand-on vessel and (iv) action required (Cockcroft and Lameijer, 2012). These stages are determined by the relative distance between the vessels and can be mapped to four corresponding levels of collision risk: no risk of collision, risk of collision, close-quarters situation and immediate danger (He et al., 2025; Wang et al., 2021). Typically, distances on the order of 5–8 nm are regarded as the outer limit of the risk-of-collision level, while 2–3 nm represent the outer boundary of a close-quarters situation.

At the first two levels of collision risk, sufficient sea-room exists for the navigator to adopt various strategies to avoid a collision. In most cases, an alteration of course is adopted. However, in multi-ship encounters, manoeuvring becomes considerably more complex. Consequently, accurate collision-avoidance simulations require the implementation of more precise manoeuvrability models. In this context, all parameters of a complete turning circle (i.e., a 720-degree turning manoeuvre) are relevant for selecting the most suitable empirical model and for assessing its performance.

At the last two levels, where the relative distance between vessels is less than 3 nm, collision avoidance typically involves applying the maximum rudder angle. Consequently, the empirical model only needs to accurately predict the vessel's trajectory up to a 90-degree course change, as trajectory predictions beyond this point are not relevant for collision risk assessment (i.e., 90-degree turning manoeuvre). Thus, in this case, the most relevant manoeuvre parameters are: advance, transfer, peak yaw rate, time required to change course by 90°, and the vessel's speed and drift at that moment.

3.5. Performance assessment

3.5.1. Accuracy and precision

Performance assessment of the simulated turning circle begins with a study of the accuracy and precision of the turning circle parameters predicted by the various polynomial regression models used to estimate empirically the hydrodynamic derivatives.

Accuracy refers to the degree to which the estimated turning circle manoeuvre parameters align with the "true" or reference values. Since the output parameters of the turning circle manoeuvre vary in scale, the mean relative error, $\overline{e_r}$, is used as the accuracy metric, see Equation (29). A lower mean relative error indicates higher accuracy, allowing for a quantitative assessment of the model's performance.

$$\overline{e_r} = \frac{1}{n}\sum_{i=1}^{n}\left|\frac{x_i - \hat{x}_i}{x_i}\right| \tag{29}$$

where, n is the number of turning circle parameters; x_i is the "true" parameter obtained from manoeuvrability tests; $\hat{x}_i$ is the estimated parameter.

Precision refers to the degree of consistency among estimates produced by repeated applications of the regression models. Since the turning circle manoeuvre results contain values of different scales, precision is assessed using the coefficient of variation, *COV*, see Equation (30). A lower *COV* indicates higher precision, whereas a higher *COV* signifies lower relative precision.

$$COV = \frac{\sigma}{\overline{e_r}} \tag{30}$$

where, σ is the standard deviation of the relative error.

To select the polynomial regression model that best estimates the

hydrodynamic derivatives for predicting the turning manoeuvre, it is essential to prioritise both accuracy and precision during the performance assessment. If the results do not clearly indicate a model that excels in both accuracy and precision, preference should be given to the model with higher accuracy.

3.5.2. Sensitivity analysis

Sensitivity analysis is performed to analyse the influence of input variables and the impact of a chosen polynomial regression model on the turning manoeuvre parameters. The analysis uses the general-propeller-rudder input variables and adopts an elasticity-based measure of sensitivity. This choice is justified by the fact that elasticity is a dimensionless ratio that quantifies the relative impact of input variables on a given output of interest. Additionally, elasticity is particularly suitable for this analysis, as the input and output variables differ in both units and magnitudes.

Elasticity is defined as the ratio of the percentage change in a turning circle parameter to the percentage change in an input variable, provided that the latter has a causal influence on the former while all other conditions remain unchanged. Mathematically, elasticity is expressed as:

$$e_i = \frac{\left(\frac{y_{i+1}-y_i}{y_i}\right)}{\left(\frac{x_{i+1}-x_i}{x_i}\right)} \tag{31}$$

where, x_i is an input variable (e.g., mass of the vessel, rudder area, propeller diameter), y_i is an output turning circle parameter (e.g., advance, transfer, drift).

Elasticity is classified into three categories. If $e > 1$, the variable is considered elastic, meaning the output parameter changes more than the input variable. If $e = 1$, the variable is unit elastic, indicating that the output parameter changes proportionally to the input. If $e < 1$, the variable is inelastic, implying that the output parameter changes less than the input variable.

3.6. Benchmark ships

Predicting ship manoeuvrability is a complex task, primarily due to the limited availability of open-access data on hydrodynamic coefficients and interaction forces. Developing a mathematical model accurately representing a vessel's real behaviour requires extensive trial data and model test results. In this study, two benchmark ship models developed by the Korea Research Institute of Ships and Ocean Engineering (KRISO) are selected for result validation: the KRISO Very Large Crude Carrier 2 (KVLCC2) and the KRISO Container Ship (KCS).

KVLCC2 is a modern tanker hull form with a bulbous bow and transom stern. KCS is a modern container ship with a bulbous bow and stern. Both were conceived in 1997. These two hull forms are among four ship models selected by the 24th ITTC Manoeuvring Committee to establish a new benchmark dataset (ITTC, 2021). Although neither vessel exists at full scale, both accurately represent modern hull designs for their respective ship types. Comprehensive geometrical data, including hydrodynamic details on the hull, propeller, rudder, and other appendages, are publicly available (see Tables 3–6).

In the simulations, the initial approach speed is set to 15.5 knots for KVLCC2 and 24 knots for KCS. The rudder steering rate is 2.33° per second, and the propeller revolution is maintained at a constant rate corresponding to the initial approach speed. The KVLCC2 manoeuvre is assessed in a starboard turning circle, while the KCS manoeuvre is assessed in a portside turning circle.

4. Results and discussion

4.1. Turning circle simulation

To validate the implemented mathematical model, the predicted motion of the two benchmark ships, KVLCC2 and KCS, is compared with available results in the literature. Both vessels are well described in the literature from the point of view of hydrodynamic coefficients and interaction forces. However, it is often difficult to find all relevant data consolidated in a single source. This is because the objectives of different studies are different, so the presented data is limited to the proposed objectives. Additionally, different studies may employ different modelling approaches, resulting in varying sets of hydrodynamic coefficients for the same vessel. In this paper, the data for both vessels were collected from multiple sources. Consequently, the validation approach serves not only to validate the accuracy of the mathematical model, but to assess whether discrepancies in input data contribute to deviations from expected outcomes, too.

4.1.1. KVLCC2

To validate the vessel manoeuvring model (VMM) and to assess the turning circle manoeuvre for KVLCC2 tanker, four different simulations are executed and the obtained results are compared in Table 7 with the data presented by MARIN (Quadvlieg and Brouwer, 2011). For comparison purposes, the trajectory path in a turning circle, the time history of speed, the time history of drift angle and the time history of yaw rate are calculated (see Fig. 6). For all case scenarios, the speed of the vessel is 15.5 knots and the rudder is deflected 35° to the starboard.

During the steady turning phase, the expected speed loss, drift angle and yaw rate closely match the values provided by MARIN, with low relative errors of 11 %, 3 % and 9 %, respectively. However, at the initial turning stage, some deviations are observed in the drift angle and yaw rate. When comparing the turning circle paths in both models, a slight deviation is noticeable after 180° of heading, though the relative error for tactical diameter and turn diameter remains below 6 %.

The minor discrepancies in the results can be attributed to variations in the input data, which were collected from different sources. Another potential source of minor discrepancies in the obtained results is scale effects in manoeuvring tests. These effects occur because the forces acting on the full-scale ship and the small-scale model (such as those from the hull, appendages and propulsors) can differ due to the model not experiencing fully turbulent flow (Barr, 1993).

The obtained results indicate that, overall, the adopted vessel manoeuvring model produces outcomes closely aligned with expected

Table 3
Principal characteristics of KVLCC2 (SIMMAN, 2020; Yasukawa and Yoshimura, 2015).

Variables	Data	Variables	Data	Variables	Data	Variables	Data
L_{PP} (m)	320	a_0	0.2931	Λ	1.826	l'_R	−0.710
B (m)	58	a_1	−0.2753	t_R	0.387	a_H	0.312
d (m)	20.8	a_2	0.1385	ε	1.09	μ'_{11}	0.022
U $(knots)$	15.5	n_P	1.2413	w_{R_0}	0.3192	μ'_{22}	0.223
m (t)	320437	w_{P_0}	0.39202	κ	0.5	μ'_{26}	0.0082
C_B	0.81	t_P	0.22	γ_R^+	0.395	μ'_{66}	0.011
x_G (m)	11.1	A_R (m^2)	136.7	γ_R^-	0.640	R'_0	0.022
D_P (m)	9.86	H_R (m)	15.8	x'_H	−0.40052		

Table 4
Hydrodynamic derivatives of KVLCC2 (Yasukawa and Yoshimura, 2015).

Variables	Data	Variables	Data	Variables	Data	Variables	Data
X'_{vv}	−0.04	Y'_{v}	−0.315	Y'_{vrr}	−0.391	N'_{vvv}	−0.03
X'_{vr}	0.002	Y'_{r}	0.083	Y'_{rrr}	0.008	N'_{vvr}	−0.294
X'_{rr}	0.011	Y'_{vvv}	−1.607	N'_{v}	−0.137	N'_{vrr}	0.055
X'_{vvvv}	0.771	Y'_{vvr}	0.379	N'_{r}	−0.049	N'_{rrr}	−0.013

Table 5
Principal characteristics of KCS (Yoshimura et al., 2008; Yoshimura and Masumoto, 2011).

Variables	Data	Variables	Data	Variables	Data	Variables	Data
L_{PP} (m)	230	a_0	0.472	Λ	1.80	l'_R	−0.755
B (m)	32.2	a_1	−0.3073	t_R	0.258	a_H	0.361
d (m)	10.8	a_2	−0.1354	ε	0.956	μ'_{11}	0.0057
U $(knots)$	24	n_P	1.7322	w_{R_0}	0.315	μ'_{22}	0.188
m (t)	53330	w_{P_0}	0.355	κ	0.633	μ'_{26}	−0.00255
C_B	0.651	t_P	0.207	γ_R^+	0.338	μ'_{66}	0.00695
x_G (m)	−3.4	A_R (m^2)	54.45	γ_R^-	0.492	R'_0	0.0167
D_P (m)	7.9	H_R (m)	9.9	x'_H	−0.436		

Table 6
Hydrodynamic derivatives of KCS (Yoshimura et al., 2008; Yoshimura and Masumoto, 2011).

Variables	Data	Variables	Data	Variables	Data	Variables	Data
X'_{vv}	−0.0549	Y'_{v}	−0.2252	Y'_{vrr}	−0.8341	N'_{vvv}	−0.1751
X'_{vr}	−0.0797	Y'_{r}	0.04705	Y'_{rrr}	−0.005	N'_{vvr}	−0.6167
X'_{rr}	−0.0120	Y'_{vvv}	−1.7179	N'_{v}	−0.1111	N'_{vrr}	−0.0512
X'_{vvvv}	−0.0417	Y'_{vvr}	−0.4832	N'_{r}	−0.0465	N'_{rrr}	−0.0387

Table 7
Comparison of experimental and predicted manoeuvring parameters obtained using the vessel manoeuvrability model for the KVLCC2.

Manoeuvring parameters	MARIN	VMM	Relative error
Time to change course 90°	4.34	4.58	0.06
Time to change course 180°	9.15	9.02	0.01
Advance	3.07	3.19	0.04
Transfer	1.36	1.43	0.06
Tactical diameter	3.28	3.32	0.01
Diameter of turn	2.50	2.36	0.06
Speed (steady turn stage)	0.36	0.32	0.11
Drift (steady turn stage)	0.32	0.33	0.003
Yaw rate (initial turn stage)	0.48	0.44	0.09
Yaw rate (steady turn stage)	0.29	0.28	0.01
		$\overline{e_r}$	0.05
		σ	0.03
		COV	0.76

values, with a mean relative error of approximately 5 % for KVLCC2. This level of error is considered acceptable for manoeuvrability simulations.

4.1.2. KCS

To validate the vessel manoeuvring model (VMM) and to assess the turning circle manoeuvre for KCS container vessel, four different simulations are executed and the obtained results are compared in Table 8 with the data presented by SIMMAN (2020). Similar to KVLCC2, the trajectory path in the turning circle, the time history of speed, the time history of drift angle and the time history of yaw rate are calculated (see Fig. 7). For all case scenarios, the speed of the vessel is 24 knots and the rudder is deflected 35° to the portside.

During the steady turning phase, the predicted speed, drift angle and yaw rate deviate by approximately 22 % from the results provided by SIMMAN, exceeding the acceptable margin of error for manoeuvrability simulations. One possible explanation for this discrepancy is the low metacentric height, where the inclusion of heel effects appears to be significant (ITTC, 2021). As a result, for the KCS ship, methods with a minimum of 4 degrees of freedom (DOF) can be preferred over 3 DOF to achieve more accurate manoeuvring predictions.

However, considering all manoeuvring parameters of the turning circle manoeuvre, the mean relative error is approximately 15 % for KCS, which is within an acceptable accuracy range for this type of assessment.

4.2. Accuracy and precision assessment of ship manoeuvring regression models

This section evaluates the accuracy and precision of the turning circle parameters predicted by various standard and hybrid polynomial regression models used for the empirical estimation of hydrodynamic derivatives. To achieve this, a turning circle manoeuvre is simulated under the assumption that all vessel data are known, except for the hydrodynamic derivatives. These derivatives are first estimated using polynomial regression models with both linear and nonlinear coefficients, namely: the Inoue model (Inoue et al., 1981), Kijima model (Kijima et al., 1990), Matsunaga model (Matsunaga, 1993), Yoshimura-03 model (Yoshimura and Ma, 2003) and Yoshimura-11 model (Yoshimura and Masumoto, 2011).

For each regression model, a turning manoeuvre is simulated based on the newly estimated hydrodynamic derivatives. Two types of manoeuvring parameters are then recorded: the key parameters of a complete turning circle and those of a turning manoeuvre up to a 90-degree course change (see Section 3.4). The mean relative error is calculated to assess accuracy, while the mean coefficient of variation is computed to evaluate precision. The objective is to determine whether there is a significant difference between the polynomial regression models when applied to different collision risk scenarios.

The same procedure is applied to hybrid polynomial regression models to assess whether integrating regression models with only linear coefficients into models with both linear and nonlinear coefficients enhances accuracy and precision. In this study, the following linear-

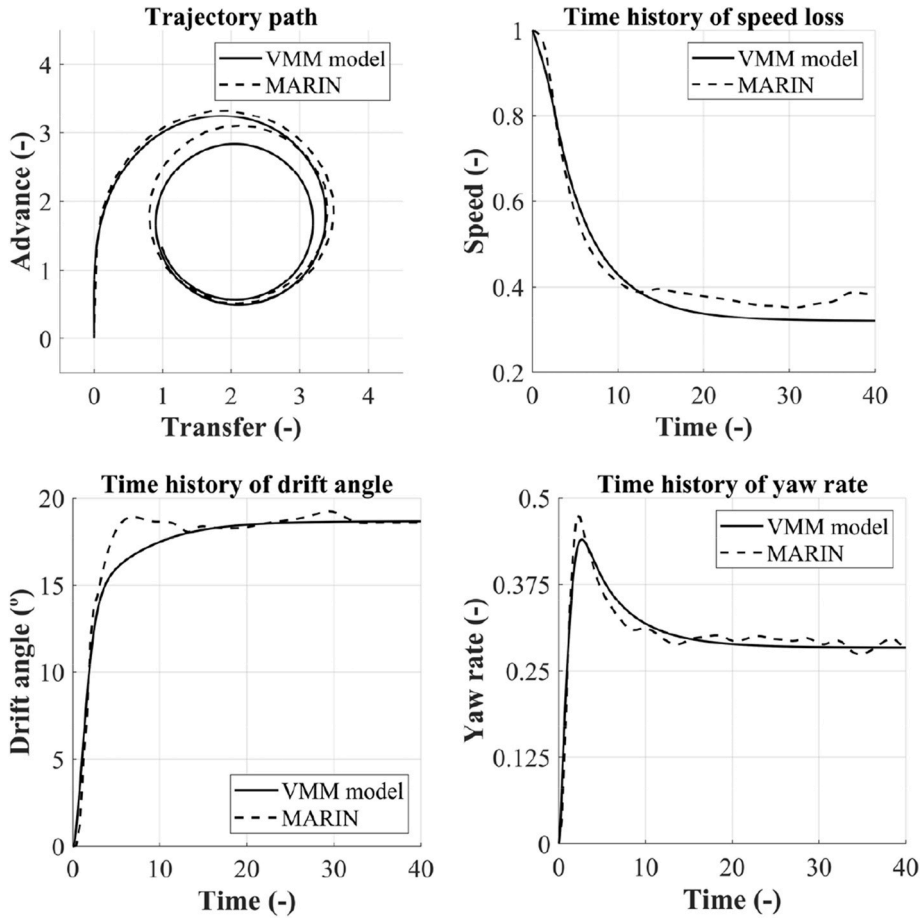

Fig. 6. Manoeuvrability measurements of KVLCC2 in steady starboard turn at 15.5 knots.

Table 8
Comparison of experimental and predicted manoeuvring parameters obtained using the vessel manoeuvrability model for the KCS.

Manoeuvring parameters	SIMMAN	VMM	Relative error
Time to change course 90°	4.46	4.67	0.05
Time to change course 180°	8.80	8.96	0.02
Advance	3.11	3.19	0.03
Transfer	1.38	1.55	0.13
Tactical diameter	3.22	3.48	0.08
Diameter of turn	2.22	2.78	0.25
Speed (steady turn stage)	0.37	0.47	0.27
Drift (steady turn stage)	0.31	0.25	0.18
Yaw rate (initial turn stage)	0.55	0.42	0.23
Yaw rate (steady turn stage)	0.43	0.34	0.22
		$\overline{e_r}$	0.15
		σ	0.09
		COV	0.63

coefficient polynomial regression models are considered: Norrbin model (Norrbin, 1971), Smitt model (Smitt, 1971), Clarke model (Clarke et al., 1983), Khattab model (Khattab, 1984) and Ankudinov model (Ankudinov, 1987).

4.2.1. *KVLCC2 in 720-degree turning manoeuvre*

Tables 9 and 10 summarise the mean relative errors and COVs of KVLCC2 720-degree turning manoeuvre parameters based on different polynomial regression models. An analysis of the standard polynomial regression models reveals that none of them exhibit both high accuracy and high precision simultaneously. Among the models, Matsunaga demonstrates the lowest mean relative error, making it the most accurate. However, it is not the most precise, as its coefficient of variation is the second highest among the models.

In contrast, Yoshimura-03 is the least reliable model for predicting the turning manoeuvre of a tanker, exhibiting the highest mean relative error (0.32) and the highest coefficient of variation (1.25), making it the least accurate and precise.

When considering only precision, the most stable models are Kijima and Yoshimura-11, both with a COV of 0.35. From an accuracy perspective, as previously mentioned, Matsunaga model is the most accurate, with a mean relative error of 0.13. However, the models of Inoue, Kijima and Yoshimura-11 also perform well, with mean relative errors between 0.13 and 0.20.

Given that no model achieves both the highest accuracy and precision, accuracy is prioritised in model selection. Therefore, at the lowest levels of collision risk simulations, if the hydrodynamic derivatives of a tanker vessel are unknown, they can be reliably estimated using the models of Inoue, Kijima, Matsunaga and Yoshimura-11. The Yoshimura-03 is not recommended for this purpose.

Regarding the hybrid polynomial regression models, the results show that integrating the linear coefficients from the Norrbin and Khattab models into the standard polynomial regression models enhances precision, while the Clarke model improves accuracy. Since accuracy is prioritised over precision, the analysis focuses on the results in Table 9. These results indicate that integrating the linear coefficients from Norrbin, Smitt and Khattab models negatively affects accuracy. While, Ankudinov model does not have a significant impact on accuracy.

Although hybridising polynomial regression models with the Clarke linear coefficients slightly improves accuracy, the percentage of improvement is minimal. This suggests that integrating purely linear hydrodynamic models does not significantly enhance the accuracy of

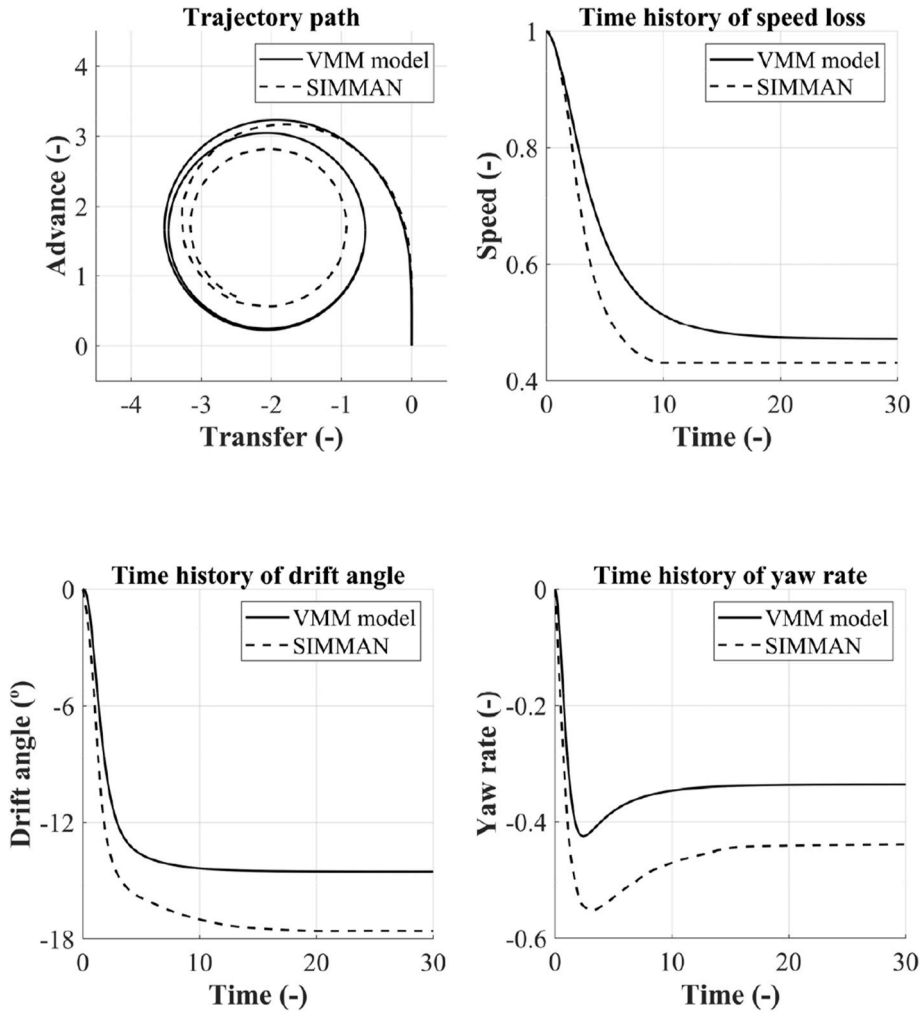

Fig. 7. Manoeuvrability measurements of KCS in a steady portside turn at 24 knots.

Table 9
Mean relative errors of KVLCC2 720-degree turning manoeuvre parameters based on different polynomial regression models.

	–	Norrbin	Smitt	Clarke	Khattab	Ankudinov
Inoue	0.17	0.27	0.39	0.16	0.29	0.19
Kijima	0.16	0.26	0.38	0.15	0.30	0.18
Matsunaga	0.13	0.21	0.22	0.11	0.24	0.13
Yoshimura-03	0.32	0.37	0.48	0.36	0.38	0.36
Yoshimura-11	0.20	0.31	0.65	0.19	0.38	0.22

Table 10
COV of KVLCC2 720-degree turning manoeuvre parameters based on different polynomial regression models.

	–	Norrbin	Smitt	Clarke	Khattab	Ankudinov
Inoue	0.53	0.35	0.82	0.96	0.37	0.88
Kijima	0.35	0.37	0.70	0.53	0.39	0.51
Matsunaga	0.58	0.45	0.83	0.61	0.51	0.48
Yoshimura-03	1.25	1.01	1.17	1.21	1.00	1.22
Yoshimura-11	0.35	0.24	0.48	0.55	0.29	0.57

Table 11
Mean relative errors of KVLCC2 90-degree turning manoeuvre parameters based on different polynomial regression models.

	–	Norrbin	Smitt	Clarke	Khattab	Ankudinov
Inoue	0.15	0.24	0.32	0.08	0.27	0.10
Kijima	0.16	0.25	0.33	0.10	0.29	0.12
Matsunaga	0.17	0.23	0.21	0.10	0.26	0.10
Yoshimura-03	0.15	0.24	0.49	0.22	0.24	0.24
Yoshimura-11	0.14	0.25	0.54	0.12	0.30	0.17

Table 12
COV of KVLCC2 90-degree turning manoeuvre parameters based on different polynomial regression models.

	–	Norrbin	Smitt	Clarke	Khattab	Ankudinov
Inoue	0.49	0.49	0.81	0.49	0.50	0.44
Kijima	0.44	0.50	0.62	0.46	0.52	0.46
Matsunaga	0.50	0.45	0.89	0.39	0.48	0.48
Yoshimura-03	0.91	0.56	1.27	0.98	0.54	1.13
Yoshimura-11	0.65	0.53	0.48	0.34	0.65	0.39

complete turning manoeuvre predictions for tanker vessels, rendering such modifications unnecessary.

4.2.2. KVLCC2 in 90-degree turning manoeuvre

Tables 11 and 12 summarise the accuracy and precision of polynomial regression models assessed based solely on turning manoeuvre parameters for up to a 90-degree course change. The results indicate that when considering only the turning manoeuvre up to a 90-degree course change, all polynomial regression models produce more accurate and precise results compared to the previous case. The models

by Inoue, Kijima, Matsunaga, Yoshimura-03, and Yoshimura-11 demonstrate high accuracy. However, for close-quarters situations, the behaviour of a tanker is better simulated using hybrid polynomial regression models.

The findings show that integrating the linear coefficients from the Clarke and Ankudinov models into standard polynomial regression models (i.e., Inoue, Kijima, Matsunaga and Yoshimura-11) significantly enhances both accuracy and precision. However, it is important to note that Yoshimura-03 is not recommended for this purpose, as its precision remains low.

4.2.3. KCS in 720-degree turning manoeuvre

The accuracy and precision assessments for complete turning manoeuvre for both standard and hybrid polynomial regression models for a container vessel are summarised in Tables 13 and 14, respectively.

As observed in the case of KVLCC2, none of the standard polynomial regression models exhibit both high accuracy and precision. Therefore, accuracy is prioritised in the analysis. According to Table 13, Inoue and Yoshimura-11 models demonstrate the highest accuracy, with a notable difference in mean relative error compared to the other models. Consequently, if the hydrodynamic derivatives of a container vessel are unknown, these two models are the preferred empirical approaches for estimating the missing data.

Regarding the hybrid polynomial regression models, none show a significant improvement in accuracy or precision compared to the standard polynomial regression models.

4.2.4. KCS in 90-degree turning manoeuvre

The accuracy and precision assessments for the turning manoeuvre corresponding to a course change of up to 90° are summarised in Tables 15 and 16, respectively.

Compared to the previous case, the regression models in this scenario demonstrate improved accuracy, although precision has slightly decreased. As shown in Table 15, the Inoue and Yoshimura-11 models exhibit the highest accuracy. Regarding the hybrid polynomial regression models, the results indicate that integrating the linear coefficients from the Clarke and Ankudinov models into Inoue and Yoshimura-11 models show a good accuracy. Additionally, incorporating the Norrbin model into the Yoshimura-11 model yields both good accuracy and precision.

4.3. Sensitivity analysis

Sensitivity analysis is conducted to evaluate how the turning circle manoeuvre parameters respond to variations in the general-propeller-rudder input variables, and how these sensitivities change when different empirical ship manoeuvring regression models are applied.

For the model to be physically meaningful, the sensitivities should reflect the true influence of the input data on ship manoeuvrability. However, integrating empirical standard and hybrid regression models into the simulations introduces a dispersion in sensitivity values associated with the input parameters.

Since the input variables represent the physical characteristics of the rudder, propeller and the ship as a whole, the introduction of empirical regression models may influence their sensitivities and, as a result, lead to simulations of the ship's physical behaviour that deviate from its actual performance.

Therefore, based on the dispersion of sensitivity outcomes, the empirical regression models whose sensitivity values are closest to the median are selected for further analysis, as these models are consistent with the expected influence of the input data and, consequently, align with expected physical behaviour.

Conversely, models that cause a significant divergence from the general trend in input variable sensitivities are excluded, as they do not adequately reflect the physical relevance of the input variables.

This assessment is performed under two different scenarios: a complete turning circle manoeuvre (i.e., 720-degree turning manoeuvre) and a turning circle manoeuvre of a vessel in a close-quarter situation (i.e., 90-degree turning manoeuvre). In both cases, the input data remain the same (see Table 1), while the output data depend on the specific objectives of the analysis (see Section 3.4).

An initial sensitivity assessment is conducted using the general-propeller-rudder input dataset, under the assumption that the hydrodynamic derivatives are known. For this purpose, the elasticity is used as a measure of sensitivity. Elasticity is quantified by individually perturbing each input variable by 10 % and measuring the resulting percentage variation in turning circle manoeuvre parameters. The mean elasticity for each input variable is subsequently computed in accordance with Equation (31). The five input variables exhibiting the highest mean elasticities are then selected for further analysis.

To simulate the vessel's turning manoeuvre, the manoeuvring model requires as input data not only general-propeller-rudder values, but hydrodynamic derivatives, too. When hydrodynamic derivatives are unknown, they must be estimated empirically, making it essential to assess how different ship manoeuvring regression models influence the elasticity of the remaining input data.

Based on the five previously identified input variables from the general-propeller-rudder dataset, each variable is analysed in combination with 5 standard polynomial regression models and 25 hybrid

Table 13
Relative errors of KCS 720-degree turning manoeuvre parameters based on different polynomial regression models.

	–	Norrbin	Smitt	Clarke	Khattab	Ankudinov
Inoue	0.13	0.20	0.22	0.14	0.28	0.14
Kijima	0.30	0.40	0.61	0.32	0.52	0.29
Matsunaga	0.41	0.53	1.32	0.43	0.71	0.41
Yoshimura-03	0.29	0.25	0.38	0.28	0.28	0.30
Yoshimura-11	0.14	0.24	0.37	0.15	0.36	0.14

Table 14
COV of KCS 720-degree turning manoeuvre parameters based on different polynomial regression models.

	–	Norrbin	Smitt	Clarke	Khattab	Ankudinov
Inoue	0.68	0.50	1.02	0.66	0.45	0.71
Kijima	0.32	0.31	0.44	0.30	0.38	0.32
Matsunaga	0.32	0.35	0.65	0.33	0.44	0.34
Yoshimura-03	0.87	0.96	1.00	0.86	0.83	0.88
Yoshimura-11	0.80	0.46	0.50	0.75	0.41	0.78

Table 15
Relative errors of KCS 90-degree turning manoeuvre parameters based on different polynomial regression models.

	–	Norrbin	Smitt	Clarke	Khattab	Ankudinov
Inoue	0.15	0.21	0.22	0.14	0.27	0.10
Kijima	0.26	0.35	0.44	0.28	0.43	0.25
Matsunaga	0.35	0.43	0.88	0.35	0.55	0.33
Yoshimura-03	0.21	0.18	0.46	0.19	0.23	0.22
Yoshimura-11	0.12	0.21	0.25	0.14	0.28	0.12

Table 16
COV of KCS 90-degree turning manoeuvre parameters based on different polynomial regression models.

	–	Norrbin	Smitt	Clarke	Khattab	Ankudinov
Inoue	0.51	0.52	0.95	0.60	0.58	0.85
Kijima	0.43	0.45	0.52	0.42	0.54	0.44
Matsunaga	0.43	0.48	0.82	0.44	0.59	0.47
Yoshimura-03	0.87	0.90	1.16	0.81	0.79	0.93
Yoshimura-11	0.75	0.35	0.46	0.66	0.45	0.72

polynomial regression models. For each combination, the elasticity is calculated. The dispersion of the resulting elasticity values is assessed using boxplots, allowing for the identification of ship manoeuvring regression models that induce elasticities in the input variables closest to the median of the overall results.

4.3.1. KVLCC2

Fig. 8 presents the input data elasticities of KVLCC2, assuming known hydrodynamic coefficients, for two scenarios: 720-degree turning manoeuvre (i.e., a complete turning circle) and a 90-degree turning manoeuvre (i.e., representative of a vessel in a close-quarter situation).

The results, presented in Fig. 8, indicate that for the KVLCC2 vessel, the elasticity of each input variable remains below 1 in both manoeuvre scenarios. This suggests that the turning manoeuvre measurements exhibit low sensitivity to variations in input data – meaning a percentage change in any input variable results in a proportionally smaller percentage change in the output.

The five input variables with the highest elasticities that are selected for the subsequent sensitivity assessment are: $\varepsilon, D_P, n_P, A_R, \kappa$ for the 720-degree turning manoeuvre; and $\varepsilon, D_P, n_P, A_R, a_0$ for the 90-degree turning manoeuvre.

4.3.2. KVLCC2 in 720-degree turning manoeuvre

Assuming the hydrodynamic coefficients are unknown, these are estimated using a set of 30 hydrodynamic regression models, comprising five standard polynomial regression models and 25 hybrid polynomial regression models. For each model employed to estimate the hydrodynamic derivatives, the input elasticities are recalculated for every input value. Fig. 9 presents the resulting boxplots illustrating the dispersion of the elasticity values. Each circular marker represents the elasticity of a given input variable for a specific polynomial regression model used in the estimation of the hydrodynamic derivatives.

The obtained results indicate that, when hydrodynamic derivatives are unknown and estimated empirically through polynomial regression models, the elasticity of each input variable increases substantially. For instance, the elasticity of the propeller diameter, D_P, rises from 0.78 to a range between 1.5 and 5.4, depending on the regression model employed. When the hydrodynamic derivatives are estimated using the Yoshimura-11combined with Smitt, the elasticities of all input variables are identified as outliers within the dataset. It is noteworthy that this hybrid model also exhibited the highest mean relative error compared to the other models, indicating it as the least accurate.

The closest polynomial regression models to the median elasticity values are those of Inoue-Norrbin, Kijima-Norrbin and Matsunaga-Khattab. Although these models are not the most accurate (see Table 9) in terms of accuracy and precision, their mean relative error and coefficient of variation (COV) remain moderate.

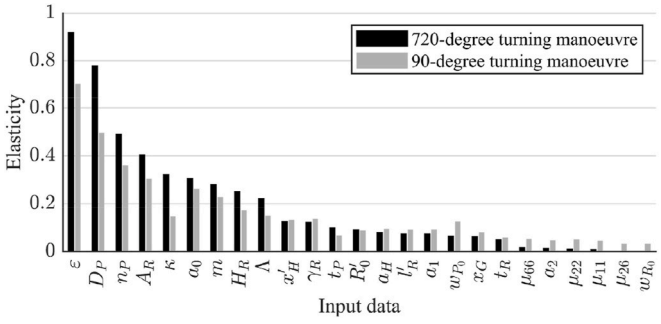

Fig. 8. Elasticity of input data for KVLCC2 in 720-degree and 90-degree turning manoeuvres.

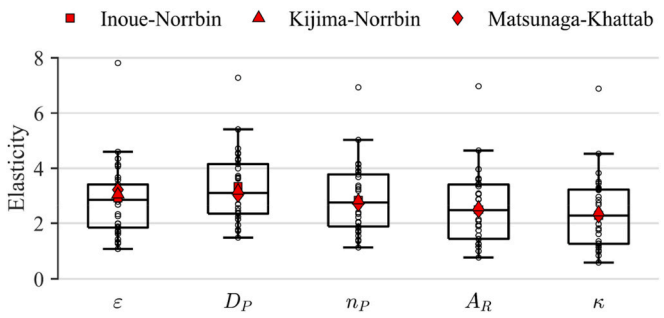

Fig. 9. Boxplots of input variable elasticities influenced by hydrodynamic derivatives from 30 polynomial regression models for KVLCC2 in 720-degree turning manoeuvre.

4.3.3. KVLCC2 in 90-degree turning manoeuvre

Fig. 10 summarises the elasticity of input variables during the 90-degree turning manoeuvre when hydrodynamic derivatives are estimated using various polynomial regression models. When employing the Yoshimura-03-Smitt or Yoshimura-11-Smitt models, the resulting input variable elasticities appear as outliers within the dataset. These models also exhibited the lowest accuracy and precision among the rest of the models (see Table 11 and Table 12). The polynomial regression models closest to the median elasticity values are those of Inoue-Norrbin, Matsunaga-Norrbin and Matsunaga-Smitt.

4.3.4. KCS

Fig. 11 presents the input data elasticities of KCS, assuming known hydrodynamic coefficients, for two scenarios: 720-degree turning manoeuvre (i.e., a complete turning circle) and a 90-degree turning manoeuvre (i.e., representative of a vessel in a close-quarter situation). As observed, the elasticity of each input variable remains below 1 in both turning manoeuvres. This indicates that turning manoeuvre parameters exhibit low sensitivity to variations in input data, meaning that a percentage change in any input variable results in a proportionally smaller percentage change in the output.

The five input variables with the highest elasticities that are selected for the subsequent sensitivity assessment are: $\varepsilon, D_P, n_P, A_R, \kappa$ for the 720-degree turning manoeuvre; and $\varepsilon, D_P, n_P, A_R, a_0$ for the 90-degree turning manoeuvre.

4.3.5. KCS – in 720-degree turning manoeuvre

Fig. 12 summarises the elasticity of input variables during the 720-degree turning manoeuvre when hydrodynamic derivatives are estimated using various polynomial regression models. When employing the Matsunaga-Smitt model, the resulting input variable elasticities appear as outliers within the dataset. This model also exhibited the lowest accuracy among the rest of the models (see Table 13).

The closest polynomial regression models to the median elasticity

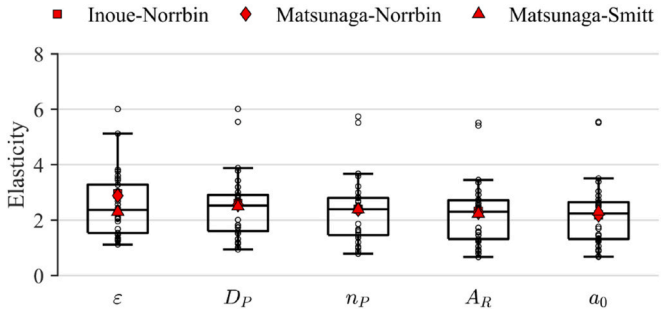

Fig. 10. Boxplots of input variable elasticities influenced by hydrodynamic derivatives from 30 polynomial regression models for KVLCC2 in 90-degree turning manoeuvre.

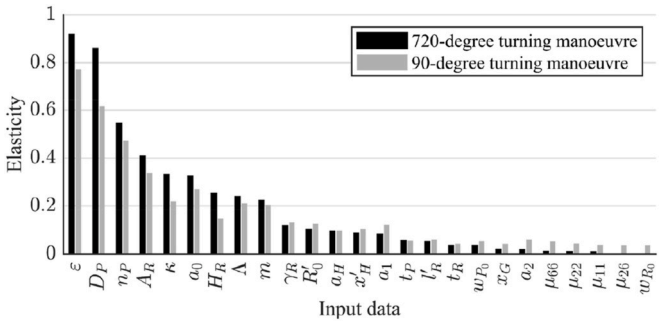

Fig. 11. Elasticity of input data for KCS in 720-degree and 90-degree turning manoeuvres.

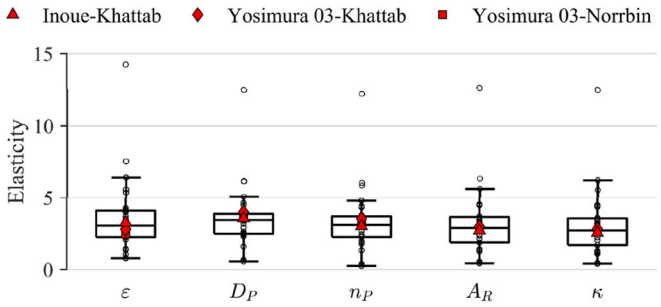

Fig. 12. Boxplots of input variable elasticities influenced by hydrodynamic derivatives from 30 polynomial regression models for KCS in 720-degree turning manoeuvre.

values are those of Inoue-Khattab, Yoshimura-03-Khattab and Yoshimura-03-Norrbin.

4.3.6. KCS – in 90-degree turning manoeuvre

Fig. 13 summarises the elasticity of input variables during the 90-degree turning manoeuvre when hydrodynamic derivatives are estimated using various polynomial regression models. When employing the Matsunaga-Smitt model, the resulting input variable elasticities appear as outliers within the dataset. This model also exhibited the lowest accuracy and precision among the rest of the models (see Tables 15 and 16).

The closest polynomial regression models to the median elasticity values are those of Inoue-Khattab, Inoue-Smitt and Yoshimura-11-Smitt.

5. Conclusions

This study assessed the performance of an empirical manoeuvrability model composed of hydrodynamic derivatives and general-propeller-rudder data, intended to serve as the foundation for a comprehensive collision risk assessment framework. Key variables influencing ship manoeuvrability were identified, with particular attention to turning circle parameters that are critical for modelling collision avoidance behaviour. Several ship manoeuvring regression models were evaluated in terms of their accuracy and precision. The sensitivity of each input variable on turning circle response was analysed using the concept of elasticity. The validation of results was carried out using two benchmark vessels: KVLCC2 and KCS.

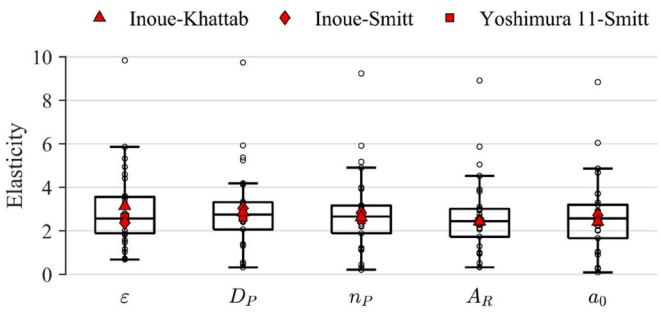

Fig. 13. Boxplots of input variable elasticities influenced by hydrodynamic derivatives from 30 polynomial regression models for KCS in 90-degree turning manoeuvre.

When two vessels approach, four collision risk levels can be identified based on relative distance. At low collision risk, when vessels are far apart, various avoidance strategies are possible, requiring all turning circle parameters for a suitable empirical model. At high collision risk, when vessels are close, maximum rudder is often used, and the model only needs to predict the trajectory up to a 90-degree course change. Key parameters then include advance, transfer, peak yaw rate, time required to change course by 90°, and the vessel's speed and drift at that moment.

The findings reveal that no single regression model, neither standard polynomial nor hybrid, achieves optimal accuracy and precision across all scenarios. As a result, model accuracy was prioritised in the selection process. For complete turning manoeuvres, standard polynomial regression models demonstrated superior accuracy. In contrast, hybrid models showed notable improvements when simulating close-quarters manoeuvres.

Therefore, at the lowest levels of collision risk simulations, if the hydrodynamic derivatives of a tanker vessel are unknown, they can be reliably estimated using the models of Inoue, Kijima, Matsunaga and Yoshimura-11. In close-quarter situations, integrating the linear coefficients from the Clarke and Ankudinov models into standard polynomial regression models (i.e., Inoue, Kijima, Matsunaga and Yoshimura-11) significantly enhances both accuracy and precision.

For a container vessel, Inoue and Yoshimura-11 models demonstrate the highest accuracy in 720-degree turning manoeuvre. For the turning manoeuvre corresponding to a course change of up to 90°, Inoue and Yoshimura-11 models exhibit the highest accuracy. Besides, the results indicate that integrating the linear coefficients from Clarke and Ankudinov models into Inoue and Yoshimura-11 models show a good accuracy, too. Additionally, incorporating the Norrbin model into the Yoshimura-11 model yields both good accuracy and precision.

The sensitivity of ship manoeuvring parameters to general-propeller-rudder input data is generally low when hydrodynamic derivatives are known, with elasticity values below one across different manoeuvre scenarios. However, when these derivatives are estimated using various polynomial regression models, the sensitivity notably increases and varies depending on the model used, with some models producing outlier elasticities linked to lower accuracy. Various regression models were identified that tend to produce elasticity values near the median with moderate errors, indicating a more balanced and reliable estimation approach.

For a tanker vessel in 720-degree turning manoeuvre, the closest polynomial regression models to the median elasticity values are those of Inoue-Norrbin, Kijima-Norrbin and Matsunaga-Khattab. Although these models are not the most accurate in terms of accuracy and precision, their mean relative error and coefficient of variation remain moderate. In 90-degree turning manoeuvre, the polynomial regression models closest to the median elasticity values are those of Inoue-Norrbin, Matsunaga-Norrbin and Matsunaga-Smitt.

For a container vessel in 720-degree turning manoeuvre, the closest polynomial regression models to the median elasticity values are those of Inoue-Khattab, Yoshimura-03-Khattab and Yoshimura-03-Norrbin. In 90-degree turning manoeuvre, there are Inoue-Khattab, Inoue-Smitt and Yoshimura-11-Smitt.

This study highlights the empirical models best suited for modern tanker and container hull forms. However, for the future research it is important to emphasise the need to refine these models to enhance their applicability to ship designs beyond traditional hull configurations.

Further studies should focus on the effects of empirically estimated input data and the inclusion of environmental influences such as shallow water, wind and currents. These factors are essential for developing a more comprehensive collision probability and risk assessment model grounded in vessel manoeuvrability characteristics.

CRediT authorship contribution statement

E. Lotovskyi: Writing – original draft, Methodology, Investigation, Formal analysis, Data curation, Conceptualization. **L. Moreira:** Writing – review & editing, Methodology, Conceptualization. **A.P. Teixeira:** Writing – review & editing, Validation, Supervision, Methodology, Funding acquisition.

Declaration of competing interest

The authors declare that they have no known competing financial interests or personal relationships that could have appeared to influence the work reported in this paper.

Acknowledgements

The first author is financed by the Portuguese Foundation for Science and Technology under contract UI/BD/154389/2022 (DOI identifier: https://doi.org/10.54499/UI/BD/154389/2022). This work contributes to the Strategic Research Plan of the Centre for Marine Technology and Ocean Engineering (CENTEC), which is financed by the Portuguese Foundation for Science and Technology under contract UIDB/UIDP/00134/2020.

Appendix A

Table A1
Nomenclature.

Variable	Meaning
a_0, a_1, a_2	Coefficients of propeller thrust open water characteristic
a_H	Rudder force increase factor
d	Design draught at full load
f_α	Gradient of the lift coefficient of rudder
l'_R	Experimental constant obtained from the captive model test to express the effective longitudinal coordinate of rudder position
m	Mass of the vessel
n_P	Number of propeller revolutions
r	Yaw rate or yaw angular velocity
$\dot{r}$	Yawing acceleration
t	Time
t_P	Thrust deduction coefficient
t_R	Steering resistance deduction factor
u	Surge velocity
$\dot{u}$	Surge acceleration
u_R	Longitudinal inflow velocity component to rudder
v	Swaying velocity
$\dot{v}$	Swaying acceleration
v_R	Lateral inflow velocity component to rudder
w_P	Effective wake fraction coefficient at propeller location in manoeuvring motion
w_{P_0}	Effective wake fraction coefficient at propeller position in straight forward motion
w_R	Effective wake fraction coefficient at rudder location in manoeuvring motion
w_{R_0}	Effective wake fraction coefficient at rudder position in straight forward motion
x_G	Longitudinal distance from the midship section to the centre of gravity of ship
x_H	Longitudinal distance from the midship section to the acting point of the additional lateral force
x_P	Longitudinal distance from the midship section to the propeller
x_R	Longitudinal distance from the midship section to the rudder position
A_R	Rudder area
B	Breadth of the vessel
C_B	Block coefficient
D_P	Propeller diameter
F_N	Rudder normal force
H_R	Rudder span
I_{zz}	Moment of inertia of a vessel relative to vertical axis
J_P	Propeller advance coefficient
K_T	Propeller thrust open water characteristic
L_{PP}	Length of the vessel measured between perpendiculars
$N'_r, N'_{rr}, N'_{rrr}, N'_v, N'_{vrr}, N'_{vv}, N'_{vvr}, N'_{vvv}$	Yaw hydrodynamic derivative
N_H	Yaw moment around midship acting on ship hull
N_R	Ship rudder moment around midship in yaw
R'_0	Coefficient of total hull resistance in calm water
T_P	Propeller thrust force
U	Speed of the vessel
U_R	Resultant inflow velocity to rudder
$X'_{rr}, X'_{vr}, X'_{vv}, X'_{vvvv}$	Surge hydrodynamic derivative
X_H	Surge force acting on ship hull
X_P	Ship propeller force in surge

(continued on next page)

Table A1 (*continued*)

Variable	Meaning
X_R	Ship rudder force in surge
Y'_r, Y'_{rr}, Y'_{rrr}, Y'_v, Y'_{vr}, Y'_{vrr}, $Y'_{vv}, Y'_{vvr}, Y'_{vvv}$	Sway hydrodynamic derivative
Y_H	Sway force acting on ship hull
Y_R	Ship rudder force in sway
α_R	Effective inflow angle to rudder
β	Hull drift angle at midship
β_P	Geometrical inflow angle to propeller in manoeuvring motions
β_R	Effective inflow angle to rudder in manoeuvring motions
γ_R	Flow straightening coefficient
δ	Rudder angle
ε	Ratio of wake fraction at propeller and rudder positions
η	Ratio of propeller diameter to rudder span
η_C	Instantaneous position of the ship along the transfer direction
κ	Experimental constant for expressing longitudinal inflow velocity component to rudder
$\mu_{11}, \mu_{22}, \mu_{26}, \mu_{66}$	Added mass
ξ_C	Instantaneous position of the ship along the advance direction
ρ	Seawater density
ψ	Heading angle of the vessel
$\dot{\psi}$	Heading rate (rate of turn)
Λ	Rudder geometric aspect ratio

Appendix B

Table B1
Empirical expressions for linear and non-linear hydrodynamic derivatives in a polynomial regression model based on Yoshimura and Ma (2003).

Hydrodynamic derivative	Empirical expression
X'_{vv}	$-0.35+0.8\frac{d}{B}$
X'_{vr}	$\mu'_{22}-m'\left(0.46-2.5\frac{d}{B}\right)$
X'_{rr}	0.03
X'_{vvvv}	$2.7-6.0\frac{d}{B}$
Y'_v	$-\left(\frac{d\,\pi}{L_{PP}}+1.4\frac{B\,C_B}{L_{PP}}\right)$
Y'_r	$\mu'_{11}+\frac{1}{2}\frac{B\,C_B}{L_{PP}}$
Y'_{vvv}	−1.2
Y'_{vvr}	−0.5
Y'_{vrr}	−0.34
Y'_{rrr}	−0.04
N'_v	$-2\frac{d}{L_{PP}}$
N'_r	$4\left(\frac{d}{L_{PP}}\right)^2-1.08\left(\frac{d}{L_{PP}}\right)$
N'_{vvv}	−0.3
N'_{vvr}	−0.33
N'_{vrr}	−0.01
N'_{rrr}	0

Table B2
Empirical expressions for linear and non-linear hydrodynamic derivatives in a polynomial regression model based on Yoshimura and Masumoto (2011).

Hydrodynamic derivative	Empirical expression
X'_{vv}	$1.15\frac{B\,C_B}{L_{PP}}-0.18$
X'_{vr}	$-\mu'_{22}+1.91\frac{B\,C_B}{L_{PP}}-0.08$

(*continued on next page*)

Table B2 (*continued*)

Hydrodynamic derivative	Empirical expression
X'_{rr}	$-0.085\frac{B\,C_B}{L_{PP}}+0.008-x'_G\,\mu'_{22}$
X'_{vvvv}	$-6.68\frac{B\,C_B}{L_{PP}}+1.1$
Y'_v	$-\left(\frac{d\,\pi}{L_{PP}}+1.4\frac{B\,C_B}{L_{PP}}\right)$
Y'_r	$\mu'_{11}+\frac{1}{2}\,\frac{B\,C_B}{L_{PP}}$
Y'_{vvv}	$-0.185\frac{L_{PP}}{B}-0.48$
Y'_{vvr}	-0.75
Y'_{vrr}	$-0.26\frac{(1-C_B)\,L_{PP}}{B}-0.11$
Y'_{rrr}	-0.051
N'_v	$-2\frac{d}{L_{PP}}$
N'_r	$4\left(\frac{d}{L_{PP}}\right)^2-1.08\left(\frac{d}{L_{PP}}\right)$
N'_{vvv}	$0.69\,C_B-0.66$
N'_{vvr}	$1.55\frac{B\,C_B}{L_{PP}}-0.76$
N'_{vrr}	$-0.075\frac{(1-C_B)\,L_{PP}}{B}+0.098$
N'_{rrr}	$\frac{1}{4}\,\frac{B\,C_B}{L_{PP}}-0.056$

Table B3
Empirical expressions for linear and non-linear hydrodynamic derivatives in a modified polynomial regression model based on Inoue et al. (1981) and completed by Sutulo and Guedes Soares (2019).

Hydrodynamic derivative	Empirical expression
X'_{vr}	$\mu'_{22}\,(1.5-1.66\,C_B)$
Y'_v	$-\left(\frac{d\,\pi}{L_{PP}}+1.4\frac{B\,C_B}{L_{PP}}\right)$
Y'_r	$\frac{1}{2}\,\frac{d\,\pi}{L_{PP}}$
Y'_{vv}	$-6.65\frac{(1-C_B)\,d}{B}+0.0735$
Y'_{vr}	$1.73\frac{(1-C_B)\,d}{B}-0.443$
Y'_{rr}	$-\frac{1}{2}\,\frac{(1-C_B)\,d}{B}$
N'_v	$-2\frac{d}{L_{PP}}$
N'_r	$4\left(\frac{d}{L_{PP}}\right)^2-1.08\left(\frac{d}{L_{PP}}\right)$
N'_{rr}	$\begin{cases} 0.675\frac{B\,C_B}{L_{PP}}-0.1015, where\ \frac{B\,C_B}{L_{PP}}\le 0.113 \\ -6.9\left(\frac{B\,C_B}{L_{PP}}-0.156\right)^2-0.012, where\ \frac{B\,C_B}{L_{PP}}>0.113 \end{cases}$
N'_{vvr}	$\begin{cases} 23.7\frac{B\,C_B}{L_{PP}}-2.23,\ where\ 0.071\le\frac{B\,C_B}{L_{PP}}\le 0.088 \\ -91.5\left(\frac{B\,C_B}{L_{PP}}\right)^2+21.15\left(\frac{B\,C_B}{L_{PP}}\right)-1.294,\ where\ 0.088<\frac{B\,C_B}{L_{PP}}\le 0.143 \\ -2.88\frac{B\,C_B}{L_{PP}}+0.268,\ where\ \frac{B\,C_B}{L_{PP}}>0.143 \end{cases}$
N'_{vrr}	$0.43\frac{C_B\,d}{B}-0.0637$

Table B4
Empirical expressions for linear and non-linear hydrodynamic derivatives in a modified polynomial regression model based on Kijima et al. (1990).

Hydrodynamic derivative	Empirical expression
X'_{vr}	$\mu'_{22}\,(1.5-1.66\,C_B)$
Y'_v	$-\left(\frac{d\,\pi}{L_{PP}}+1.4\frac{B\,C_B}{L_{PP}}\right)$

(*continued on next page*)

Table B4 (*continued*)

Hydrodynamic derivative	Empirical expression
Y'_r	$(m' + \mu'_{11}) - \frac{3}{2}\frac{B\,C_B}{L_{PP}}$
Y'_{vv}	$-2.5\frac{(1-C_B)\,d}{B} - 0.5$
Y'_{rr}	$-0.343\frac{C_B\,d}{B} + 0.07$
Y'_{vvr}	$1.5\frac{C_B\,d}{B} - 0.65$
Y'_{vrr}	$-5.95\frac{(1-C_B)\,d}{B}$
N'_v	$-2\frac{d}{L_{PP}}$
N'_r	$4\left(\frac{d}{L_{PP}}\right)^2 - 1.08\left(\frac{d}{L_{PP}}\right)$
N'_{vv}	$0.96\frac{(1-C_B)\,d}{B} - 0.066$
N'_{rr}	$0.5\frac{C_B\,B}{L_{PP}} - 0.09$
N'_{vvr}	$-57.5\left(\frac{B\,C_B}{L_{PP}}\right)^2 + 18.4\left(\frac{B\,C_B}{L_{PP}}\right) - 1.6$
N'_{vrr}	$\frac{1}{2}\frac{C_B\,d}{B} - 0.05$

Table B5
Empirical expressions for linear and non-linear hydrodynamic derivatives in a modified polynomial regression model based on Matsunaga (1993).

Hydrodynamic derivative	Empirical expression
X'_{vr}	$\mu'_{22}\,(1.5 - 1.66\,C_B)$
Y'_v	$-\left(\frac{d\,\pi}{L_{PP}} + 1.4\frac{B\,C_B}{L_{PP}}\right)$
Y'_r	$\frac{1}{2}\frac{d\,\pi}{L_{PP}}$
Y'_{vv}	$-2.5\frac{(1-C_B)\,d}{B} - 0.5$
Y'_{rr}	$-0.343\frac{C_B\,d}{B} + 0.07$
Y'_{vvr}	$-114\left(\frac{C_B\,d}{B}\right)^2 + 62.12\left(\frac{C_B\,d}{B}\right) - 8.2$
Y'_{vrr}	$-5.95\frac{(1-C_B)\,d}{B}$
N'_v	$-2\frac{d}{L_{PP}}$
N'_r	$4\left(\frac{d}{L_{PP}}\right)^2 - 1.08\left(\frac{d}{L_{PP}}\right)$
N'_{vv}	$-78\left(\frac{(1-C_B)\,d}{B}\right)^2 + 19\,\frac{(1-C_B)\,d}{B} - 1$
N'_{rr}	$0.473\frac{C_B\,B}{L_{PP}} - 0.089$
N'_{vvr}	$-120\left(\frac{B\,C_B}{L_{PP}}\right)^2 + 35.22\left(\frac{B\,C_B}{L_{PP}}\right) - 2.72$
N'_{vrr}	$\frac{1}{2}\frac{C_B\,d}{B} - 0.05$

Table B6
Empirical expressions for linear hydrodynamic derivatives based on Norrbin (1971).

Hydrodynamic derivative	Empirical expression
Y'_v	$-1.69\frac{d\,\pi}{L_{PP}} - 0.08\frac{B\,C_B}{L_{PP}}$
Y'_r	$0.645\frac{d\,\pi}{L_{PP}} - 0.36\frac{B\,C_B}{L_{PP}}$
N'_v	$-0.64\frac{d\,\pi}{L_{PP}} + 0.04\frac{B\,C_B}{L_{PP}}$
N'_r	$-0.47\frac{d\,\pi}{L_{PP}} + 0.18\frac{B\,C_B}{L_{PP}}$

Table B7
Empirical expressions for linear hydrodynamic derivatives based on Smitt (1971).

Hydrodynamic derivative	Empirical expression
Y'_v	$-5\left(\frac{d}{L_{PP}}\right)^2$
Y'_r	$1.02\left(\frac{d}{L_{PP}}\right)^2$
N'_v	$-1.95\left(\frac{d}{L_{PP}}\right)^2$
N'_r	$-0.001-0.65\left(\frac{d}{L_{PP}}\right)^2+2\,x'_G\,\frac{d\,B\,C_B}{L_{PP}^2}$

Table B8
Empirical expressions for linear hydrodynamic derivatives based on Clarke et al. (1983).

Hydrodynamic derivative	Empirical expression
Y'_v	$-\frac{d\,\pi}{L_{PP}}\left(1+0.4\frac{B\,C_B}{d}\right)$
Y'_r	$-\frac{d\,\pi}{L_{PP}}\left(-\frac{1}{2}+2.2\frac{B}{L_{PP}}-0.08\frac{B}{d}\right)$
N'_v	$-\frac{d\,\pi}{L_{PP}}\left(\frac{1}{2}+2.4\frac{d}{L_{PP}}\right)$
N'_r	$-\frac{d\,\pi}{L_{PP}}\left(\frac{1}{4}+0.039\frac{B}{d}-0.56\frac{B}{L_{PP}}\right)$

Table B9
Empirical expressions for linear hydrodynamic derivatives based on Khattab (1984).

Hydrodynamic derivative	Empirical expression
Y'_v	$-2.3\frac{d}{L_{PP}}-1.466\frac{B\,C_B}{L_{PP}}+0.00102\frac{L_{PP}}{d}$
Y'_r	$1.0328\frac{d}{L_{PP}}+0.11\frac{B\,C_B}{L_{PP}}+0.00004\frac{L_{PP}}{d}$
N'_v	$-1.758\frac{d}{L_{PP}}+0.00768\frac{C_B\,L_{PP}}{B}+0.0008\frac{L_{PP}}{d}$
N'_r	$-1.3192\frac{d}{L_{PP}}+0.68228\frac{C_B\,d}{L_{PP}}+0.00019\frac{L_{PP}}{d}$

Table B10
Empirical expressions for linear hydrodynamic derivatives based on Ankudinov (1987).

Hydrodynamic derivative	Empirical expression
Y'_v	$-\frac{d\,\pi}{L_{PP}}K_y\left(0.25\left(\frac{B\,C_B}{d}\right)^2-1.5\left(\frac{B\,C_B}{d}\right)+3.45\right)$, *where if* $\frac{B\,C_B}{d}>5\Rightarrow K_y=5\frac{d}{B\,C_B}$; *else* $K_y=1$
Y'_r	$-\frac{d\,\pi}{L_{PP}}\left(-0.3+\frac{B\,C_B}{L_{PP}}+Y'_v\right)$
N'_v	$-0.75\frac{d\,\pi}{L_{PP}}+0.04\frac{B\,C_B}{L_{PP}}$
N'_r	$-\frac{d\,\pi}{L_{PP}}K_y\left(0.03\left(\frac{B\,C_B}{d}\right)^2-0.15\frac{B\,C_B}{d}+0.5\right)$, *where if* $\frac{B\,C_B}{d}>5\Rightarrow K_y=5\frac{d}{B\,C_B}$; *else* $K_y=1$

References

Abilio Ramos, M., Utne, I.B., Mosleh, A., 2019. Collision avoidance on maritime autonomous surface ships: operators' tasks and human failure events. Saf. Sci. 116, 33–44. https://doi.org/10.1016/j.ssci.2019.02.038.

Abkowitz, M.A., 1964. Lectures on ship hydrodynamics - steering and manoeuvrability. Hydro- og Aerodynamisk Laboratorium.

ABS, 2006. Guide for vessel maneuverability. Am. Bureau Ship. (ABS).

Ankudinov, V., 1987. Controllability assessment using prediction techniques. Design Workbook on Ship Maneuverability.

Aoki, I., Kijima, K., Furukawa, Y., Nakiri, Y., 2006. On the prediction method for maneuverability of a full scale ship. J. Jpn. Soc. Nav. Archit. Ocean Eng. 3 (0), 157–165. https://doi.org/10.2534/jjasnaoe.3.157.

Aram, S., Silva, K.M., 2019. Computational fluid dynamics prediction of hydrodynamic derivatives for maneuvering models of a fully-appended ship. Proceedings of the 17th International Ship Stability Workshop, pp. 57–66.

Araújo, J.P., Moreira, L., Guedes Soares, C., 2021. Modelling ship manoeuvrability using Recurrent Neural Networks. In: Developments in Maritime Technology and Engineering, first ed. CRC Press, pp. 131–139. https://doi.org/10.1201/9781003216599-15.

Balagopalan, A., Tiwari, K., Rameesha, T.V., Krishnankutty, P., 2020. Manoeuvring prediction of a container ship using the numerical PMM test and experimental validation using the free running model test. Ships Offshore Struct. 15 (8), 852–865. https://doi.org/10.1080/17445302.2019.1688921.

Baldauf, M., Mehdi, R., Deeb, H., Schröder-Hinrichs, J.U., Benedict, K., Krüger, C., Fischer, S., Gluch, M., 2015. Manoeuvring areas to adapt ACAS for the maritime domain. Zeszyty Naukowe Akademii Morskiej w Szczecinie 43 (115), 39–47.

Barr, R.A., 1993. A Review and Comparison of Ship Maneuvering Simulation Methods, 101. Transactions of the Society of Naval Architects and Marine Engineers, pp. 609–635.

Chaal, M., Ren, X., BahooToroody, A., Basnet, S., Bolbot, V., Banda, O.A.V., Gelder, P. Van, 2023. Research on risk, safety, and reliability of autonomous ships: a bibliometric review. Saf. Sci. 167, 106256. https://doi.org/10.1016/j.ssci.2023.106256.

Cho, Y.R., Yoon, B.S., Yum, D.J., Lee, M.S., 2007. Prediction of ship manoeuvrability in initial design stage using CFD based calculation. J. Ship Ocean Technol. 11 (1), 11–24.

Clarke, D., Gedling, P., Hine, G., 1983. The Application of Manoeuvring Criteria in Hull Design Using Linear Theory, 125. Transactions of the Royal Institution of Naval Architects, pp. 45–68.

Cockcroft, A.N., Lameijer, J.N.F., 2012. A Guide to the Collision Avoidance Rules: International Regulations for Preventing Collisions at Sea. Elsevier.

Čorić, M., Mandžuka, S., Gudelj, A., Lušić, Z., 2021. Quantitative ship collision frequency estimation models: a review. J. Mar. Sci. Eng. 9 (5). https://doi.org/10.3390/jmse9050533. MDPI AG.

Fan, C., Wróbel, K., Montewka, J., Gil, M., Wan, C., Zhang, D., 2020. A framework to identify factors influencing navigational risk for Maritime Autonomous Surface Ships. Ocean Eng. 202, 107188. https://doi.org/10.1016/j.oceaneng.2020.107188.

Fossen, T.I., 2011. Handbook of Marine Craft Hydrodynamics and Motion Control, first ed. John Wiley & Sons, Ltd.

Fujii, H., 1960. Experimental researches on rudder performance. J. Zosen Kiokai 107, 105–111.

Gil, M., 2021. A concept of critical safety area applicable for an obstacle-avoidance process for manned and autonomous ships. Reliab. Eng. Syst. Saf. 214, 107806. https://doi.org/10.1016/j.ress.2021.107806.

Go, G., Ahn, H.T., 2019. Hydrodynamic derivative determination based on CFD and motion simulation for a tow-fish. Appl. Ocean Res. 82, 191–209. https://doi.org/10.1016/j.apor.2018.10.023.

He, Z., Liu, C., Yan, R., Chu, X., 2025. A novel arena-based collision avoidance behavior analysis method for autonomous ships. Ocean Eng. 339, 122056. https://doi.org/10.1016/j.oceaneng.2025.122056.

Hörteborn, A., Ringsberg, J.W., 2021. A method for risk analysis of ship collisions with stationary infrastructure using AIS data and a ship manoeuvring simulator. Ocean Eng. 235, 109396. https://doi.org/10.1016/j.oceaneng.2021.109396.

IMO, 2002. Adopted on 4 December 2002. Annex 6. Standards for Ship Manoeuvrability. Resolution MSC Int. Maritime Org. (IMO) 137 (76).

Inoue, S., Hirano, M., Kijima, K., 1981. Hydrodynamic derivatives on ship manoeuvring. Int. Shipbuild. Prog. 28 (321), 112–125.

Iseki, T., 2019. Real-time estimation of the ship manoeuvrable range in wind. Ocean Eng. 190, 106396. https://doi.org/10.1016/j.oceaneng.2019.106396.

Islam, H., Guedes Soares, C., 2018. Estimation of hydrodynamic derivatives of a container ship using PMM simulation in OpenFOAM. Ocean Eng. 164, 414–425. https://doi.org/10.1016/j.oceaneng.2018.06.063.

ITTC, 2008. The manoeuvring committee. Final report and recommendations to the 25th ITTC. In: Proceedings of the 25th International Towing Tank Conference (ITTC), I.

ITTC, 2021. Guideline. Benchmark data for validation of manoeuvring predictions. In: *ITTC Quality System Manual. Recommended Procedures and Guidelines*. International Towing Tank Conference (ITTC).

Jensen, S., Lützen, M., Mikkelsen, L.L., Rasmussen, H.B., Pedersen, P.V., Schamby, P., 2018. Energy-efficient operational training in a ship bridge simulator. J. Clean. Prod. 171, 175–183. https://doi.org/10.1016/j.jclepro.2017.10.026.

Khattab, O., 1984. Multiple regression analysis of the hydrodynamic derivatives for manoeuvring equations. British Ship Res. Assoc. (BSRA) W1090.

Kijima, K., Nakiri, Y., Katsuno, T., Furukawa, Y., 1990. On the manoeuvring performance of a ship with the parameter of loading condition. Soc. Naval Architect. Japan 168, 141–148.

Krata, P., Montewka, J., 2015. Assessment of a critical area for a give-way ship in a collision encounter. Archiv. Transp. 34 (2), 51–60. https://doi.org/10.5604/08669546.1169212.

Li, M., Mou, J., Chen, L., He, Y., Huang, Y., 2021. A rule-aware time-varying conflict risk measure for MASS considering maritime practice. Reliab. Eng. Syst. Saf. 215, 107816. https://doi.org/10.1016/j.ress.2021.107816.

Li, S., Liu, J., Negenborn, R.R., 2019. Distributed coordination for collision avoidance of multiple ships considering ship maneuverability. Ocean Eng. 181, 212–226. https://doi.org/10.1016/j.oceaneng.2019.03.054.

Lotovskyi, E., Rong, H., Teixeira, A.P., 2024. Collision risk assessment in ship encounter scenarios using AIS trajectory data. In: Guedes Soares, C., Santos, T. (Eds.), Advances in Maritime Technology and Engineering. CRC Press, pp. 135–142. https://doi.org/10.1201/9781003508762-17.

Lotovskyi, E., Teixeira, A.P., 2023. Effect of timely manoeuvre execution on the collision probability in head-on and crossing encounter scenarios. In: Le Sourne, H., Guedes Soares, C. (Eds.), Advances in the Collision and Grounding of Ships and Offshore Structures. CRC Press, pp. 113–120. https://doi.org/10.1201/9781003462170-16.

Matsunaga, M., 1993. Method of predicting ship manoeuvrability in deep and shallow waters as a function of loading connection. Tech. Bullet. Nippon Kaiji Kyokai 11, 51–59.

Mehdi, R.A., Baldauf, M., Deeb, H., 2020. A dynamic risk assessment method to address safety of navigation concerns around offshore renewable energy installations. Proc. IME M J. Eng. Marit. Environ. 234 (1), 231–244. https://doi.org/10.1177/1475090219837409.

Mohovic, D., Mohovic, R., Suljic, M., Njegovan, M., 2021. Reducing the risk of collision between ships in a close-quarters situation by simulating collision avoidance actions. J. Navig. 74 (3), 558–573. https://doi.org/10.1017/S0373463321000114.

Montewka, J., Hinz, T., Kujala, P., Matusiak, J., 2010. Probability modelling of vessel collisions. Reliab. Eng. Syst. Saf. 95 (5), 573–589.

Moreira, L., Guedes Soares, C., 2022. Simulating ship manoeuvrability with artificial neural networks trained by a short noisy data set. J. Mar. Sci. Eng. 11 (1), 15. https://doi.org/10.3390/jmse11010015.

Moreira, L., Guedes Soares, C., 2024. Investigation of vessel manoeuvring abilities in shallow depths by applying neural networks. J. Mar. Sci. Eng. 12 (9), 1664. https://doi.org/10.3390/jmse12091664.

Nomoto, K., Taguchi, T., Honda, K., Hirano, S., 1957. On the steering qualities of ships. Int. Shipbuild. Prog. 4 (35), 354–370. ISP.

Norrbin, N., 1971. Theory and observations on the use of a mathematical model for ship manoeuvring in deep and confined waters. Swedish State Shipbuild. Experiment. Tank 68.

Oltmann, P., 2003. Identification of hydrodynamic damping derivatives - a pragmatic approach. International Conference on Marine Simulation and Ship Maneuverability (MARSIM'03).

Pires da Silva, P., Sutulo, S., Guedes Soares, C., 2023. Sensitivity analysis of ship manoeuvring mathematical models. J. Mar. Sci. Eng. 11 (2), 416. https://doi.org/10.3390/jmse11020416.

Quadvlieg, F., Brouwer, J., 2011. KVLCC2 benchmark data including uncertainty analysis to support manoeuvring predictions. In: Eça, L., Oñate, E., García, J., Kvamsdal, T., Bergan, P. (Eds.), International Conference on Computational Methods in Marine Engineering (MARINE 2011).

Rong, H., Teixeira, A.P., Guedes Soares, C., 2022. Ship collision avoidance behaviour recognition and analysis based on AIS data. Ocean Eng. 245, 110479. https://doi.org/10.1016/j.oceaneng.2021.110479.

Schneekluth, H., 1987. Ship Design for Efficiency and Economy, first ed. Butterworths.

Senol, Y.E., Seyhan, A., 2024. A novel machine-learning based prediction model for ship manoeuvring emissions by using bridge simulator. Ocean Eng. 291, 116411. https://doi.org/10.1016/j.oceaneng.2023.116411.

Silveira, P., Teixeira, A., Guedes Soares, C., 2016. Probabilistic modelling of evasive manoeuvring actions to avoid collisions. In: Guedes Soares, C., Santos, T. (Eds.), Maritime Technology and Engineering III. CRC Press, pp. 887–893.

SIMMAN, 2020. Official website of workshop on verification and validation of ship manoeuvring simulation methods. SIMMAN 2020. . https://www.simman2020.kr/. Accessed: 2025-03-25.

Smitt, L.W., 1971. Steering and manoeuvring of ships - full scale and model tests. Europ. Shipbuild. 20 (1).

SNAME, 1989. Principles of naval architecture. In: Lewis, E.V. (Ed.), Motions in Waves and Controllability, second ed. III. The Society of Naval Architects and Marine Engineers.

Sukas, O.F., Kinaci, O.K., Bal, S., 2019. Theoretical background and application of MANSIM for ship maneuvering simulations. Ocean Eng. 192, 106239. https://doi.org/10.1016/j.oceaneng.2019.106239.

Sutulo, S., Guedes Soares, C., 2011. Mathematical models for simulation of manoeuvring performance of ships. In: Guedes Soares, C., Garbatov, Y., Fonseca, N., Teixeira, A.P. (Eds.), Marine Technology and Engineering. Taylor & Francis Group, pp. 661–698.

Sutulo, S., Guedes Soares, C., 2019. On the application of empiric methods for prediction of ship manoeuvring properties and associated uncertainties. Ocean Eng. 186, 106111. https://doi.org/10.1016/j.oceaneng.2019.106111.

Sutulo, S., Guedes Soares, C., 2024. Nomoto-type manoeuvring mathematical models and their applicability to simulation tasks. Ocean Eng. 304, 117639. https://doi.org/10.1016/j.oceaneng.2024.117639.

Szlapczynski, R., Krata, P., Szlapczynska, J., 2018. Ship domain applied to determining distances for collision avoidance manoeuvres in give-way situations. Ocean Eng. 165, 43–54. https://doi.org/10.1016/j.oceaneng.2018.07.041.

Taimuri, G., Matusiak, J., Mikkola, T., Kujala, P., Hirdaris, S., 2020. A 6-DoF maneuvering model for the rapid estimation of hydrodynamic actions in deep and shallow waters. Ocean Eng. 218, 108103. https://doi.org/10.1016/j.oceaneng.2020.108103.

Wang, B., He, Y., Hu, W., Mou, J., Li, L., Zhang, K., Huang, L., 2021. A decision-making method for autonomous collision avoidance for the Stand-On vessel based on motion process and COLREGs. J. Mar. Sci. Eng. 9 (6), 584. https://doi.org/10.3390/jmse9060584.

Wang, T., Wu, Q., Zhang, J., Wu, B., Wang, Y., 2020. Autonomous decision-making scheme for multi-ship collision avoidance with iterative observation and inference. Ocean Eng. 197, 106873. https://doi.org/10.1016/j.oceaneng.2019.106873.

Yasukawa, H., Yoshimura, Y., 2015. Introduction of MMG standard method for ship maneuvering predictions. J. Mar. Sci. Technol. 20 (1), 37–52. https://doi.org/10.1007/s00773-014-0293-y.

Yeo, D.J., Yun, K., Kim, Y.G., 2018. A study on the effect of heel angle on maneuvering characteristics of KCS. Proceedings of the International Conference on Ship Manoeuvrability and Maritime Simulation (MARSIM 2018).

Yoshimura, Y., Ma, N., 2003. Manoeuvring prediction of fishing vessels. International Conference on Marine Simulation and Ship Manoeuvrability 2003 (MARSIM'03), pp. 793–802.

Yoshimura, Y., Masumoto, Y., 2011. Hydrodynamic force database with medium high speed merchant ships including fishing vessels and investigation into a manoeuvring prediction method. J. Jpn. Soc. Nav. Archit. Ocean Eng. 14, 63–73. https://doi.org/10.2534/jjasnaoe.14.63.

Yoshimura, Y., Ueno, M., Tsukada, Y., 2008. Analysis of steady hydrodynamic force components and prediction of manoeuvring ship motion with KVLCC1, KVLCC2 and KCS. Workshop on Verification and Validation of Ship Manoeuvring Simulation Method (SIMMAN 2008). Workshop Proceedings, pp. 80–86.

Yun, K., Yeo, D.J., Kim, D.J., 2018. An experimental study on the turning characteristics of KCS with CG variations. Proceedings of the International Conference on Ship Manoeuvrability and Maritime Simulation (MARSIM 2018).